2016

Feasibility Study of Energy Storage Technologies for Remote Microgrid's Energy Management System

Md Habib Ullah
South Dakota State University

FEASIBILITY STUDY OF ENERGY STORAGE TECHNOLOGIES FOR REMOTE MICROGRID'S ENERGY MANAGEMENT SYSTEM

BY

MD HABIB ULLAH

A thesis submitted in partial fulfillment of the requirements for the

Master of Science

Major in Electrical Engineering

South Dakota State University

2016

FEASIBILITY STUDY OF ENERGY STORAGE TECHNOLOGIES FOR REMOTE MICROGRID'S ENERGY MANAGEMENT SYSTEM

This thesis is approved as a creditable and independent investigation by a candidate for the Master of Science in Electrical Engineering degree and is acceptable for meeting the thesis requirements for this degree. Acceptance of this thesis does not imply that the conclusions reached by the candidates are necessarily the conclusions of the major department.

Reinaldo Tonkoski, Ph.D.
Major Advisor Date

Steven Hietpas, Ph.D.
Head, Electrical Engineering and Computer Science Date

Dean, Graduate School Date

ACKNOWLEDGEMENTS

Firstly, I would like to express my heartiest appreciation to my research supervisor Dr. Reinaldo Tonkoski for his continuous support and motivation not only in research but also in academic activities during my Master studies. Completion of my thesis could not have been accomplished without his encouragement from the beginning of my journey. I am also thankful to Dr. David Galipeau and Dr. Wei Sun for their motivation at the early stages of my abroad life.

Besides my supervisor, I would like to offer my gratitude to all of my course instructors and my thesis committee members for their valuable suggestions towards successful completion of my master degree. I am also grateful for the research and learning opportunities provided by the Electrical Engineering and Computer Science Department, South Dakota State University.

My sincere thanks also goes to Mr. Santosh Chalise. His suggestions and motivational speech helped me a lot to overcome my hard time in research. Abu Mitul, Ali, Ayush, Bijen, Dipesh, Lal, Riaz, Sadhana, Shaili, Shiva, Tamal and Venkat also deserve my appreciation for their continuous support in my research and academics.

Finally, I would like thank my family members for their unconditional support and love. Without their support even it was not possible to start my Master study. Thank you all whoever helped me to go through a smooth way to achieve my dream.

CONTENTS

LIST OF FIGURES

LIST OF TABLES

ABSTRACT

FEASIBILITY STUDY OF ENERGY STORAGE TECHNOLOGIES FOR REMOTE MICROGRID'S ENERGY MANAGEMENT SYSTEM

MD HABIB ULLAH

2016

Energy storage systems (ESSs) play a significant role in remote microgrids energy management system (EMS) with the large penetration rate of renewable energy which is intermittent in nature. Energy storage improves system reliability and efficiency in remote microgrids by optimizing the power demand and generation to reduce operational costs. Moreover, it increases the dispatch ability of the energy sources in remote microgrid systems. Lead acid battery (PbA) can be used as an energy storage device in remote microgrids due to its low cost; however, the response rate, short life cycle, and depth of discharge (DoD) lead to high operational costs. Ultracapacitor has a considerably longer life cycle, its energy density is low, and the initial cost is very high. Lithium-ion (Li-ion) and hybrid ion batteries may have comparatively better economical prospects in terms of DoD, life cycle, and operational cost. In this thesis, different energy storage technologies are considered for remote microgrids energy management systems. In addition, the Schiffer weighted Ah throughput model introduces two weight factors to describe that a battery degrades faster in real time operation than the standard test conditions due to different stress factors. These weight factors virtually increase the battery throughput, and accelerate the degradation. To mitigate this problem, different periodical and auto cycling strategies were investigated in this thesis. However, the results demonstrated that frequent

full charging prevents the battery from over degradation. Auto cycling strategy was found more cost effective than the periodical cycling. Applying this cycling strategy, the yearly total operational cost of a microgrid system with a 142 kWh PbA battery bank was reduced by 0.62% ($826). Results also showed that the wear cost is an important factor to consider while designing the energy management system. Li-ion and hybrid-ion batteries had lower wear costs and showed great potentiality, although the EMS with a Li-ion battery was found to be 2.55% more cost effective and 1.5% more fuel efficient than hybrid ion batteries. The reduction in operational cost ensures the access to low cost electricity for the people in remote areas. It will accelerate the development of industries, communications, technologies, and the standard of living including the remote health clinics in those areas. Furthermore, the reduction in generators fuel consumption will reduce CO_2 emission which will lower the global warming and the greenhouse effect. In this thesis, one of the objectives was to prolong the battery lifetime by preventing the degradation, that may lower the number of yearly battery disposals which are hazardous to the human health and the environment.

CHAPTER 1 INTRODUCTION

1.1 Background

The global electricity demand is increasing day by day with the high population growth rate. Electrical energy is a significant factor for global development. Lack of reliable access to electricity is a barrier towards the development [1]. Presently, 17% of the global population lives without access to electricity, and around 80% of this population lives in rural areas [2]. To ensure development in remote areas, microgrid system is one of the most viable solutions wherein renewable energy sources are integrated with fossil fuel based power generation system.

Currently, diesel generators are considered as a primary energy source in over 4,000 remote microgrids [3], and this is due to availability, low investment cost, and easy transportability since the remote microgrids generators are typically small in size. In remote microgrids, loads are highly variable and diesel generators are typically sized to meet the peak load demand although the ratio of peak to average load ratio is high as of 4-10 [4]. High-fuel efficiency of diesel generators is obtained near to rated load and it is lower in the low-loading condition. It is recommended by the manufacturers not to operate diesel generators in low (typically, less than 30% of rated load) loading condition to avoid wet stacking, fuel dilution, and carbon build up [5]. However, integration of renewable energy in the remote microgrids further reduces the diesel generator loading as well as the efficiency. Moreover, renewable energy sources are intermittent in nature which are unlike the displaceable sources in power generation that led to concern regarding the reliability of the system. Traditionally, generators minimum loading is maintained by using low cost

dump loads or by PV power curtailment in the system. However, energy is being wasted in either approach. Moreover, there is a waste of costly fuel in case of using dump load. To mitigate the aforementioned problems, energy storage systems (ESSs) are being used in remote microgrids [6]. Locally, it improves the energy management system (EMS) of remote microgrids, and reduces fuel consumption of the generators. Moreover, ESS helps EMS to utilize maximum renewable energy sources in the system.

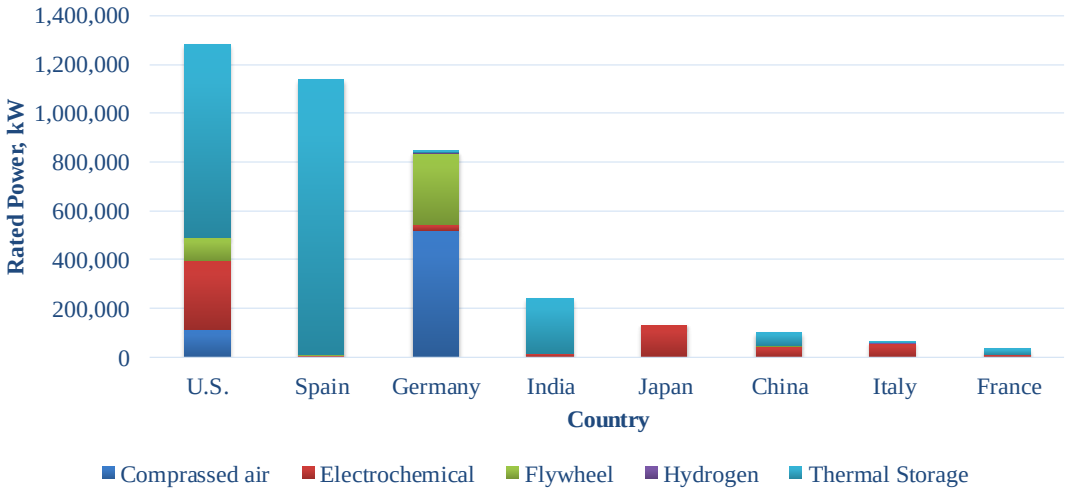

Figure 1.1. Energy storage (without pumped hydro) technology handled by country [7]

ESS provides a wide array of technological approaches according to the form of energy it contains. Presently, 95% of worldwide total installed energy storage technology is pumped hydro which is one of the oldest and most prominent storage system [8]. The remaining 5% belongs to other storage technologies, such as batteries, flywheels, ultracapacitors, compressed air, thermal storage, and so on. Lead acid (PbA) battery is the first form of rechargeable battery, and it has been commonly used as secondary energy storage device for almost 150 years [9]. High energy density, low maintenance, and comparatively lower initial price ($/kWh) features of the lead acid battery make it more

competitive in different power applications; however, its response rate is cooperatively slow; it has a short life cycle, and recommended DoD (usually 50%) leads to higher system operational cost. Currently, lithium-ion (Li-ion) batteries are being deployed more than other storage systems (Figure 1.2) in large scale grid applications and microgrids. Li-ion batteries have a high life cycle at rated DoD compared to the PbA batteries, but the initial cost of energy ($/kWh) is higher than the PbA battery. Another energy storage technology, UC, has up to 1,000,000 life cycles with 10 years of lifetime [10]. Compared to the other storage technologies, UC has a faster response rate, but low energy density and high initial cost are its main disadvantages. In recent years, hybrid ion technology is emerging as its operational cost, life cycle and allowable DoD is compatible with Li-ion technology.

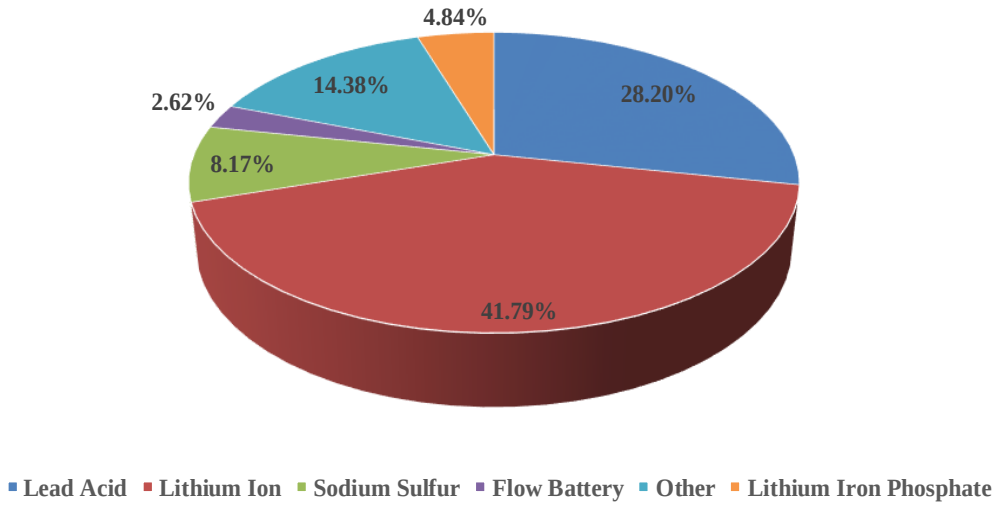

Figure 1.2. Energy storage technology deployed onto the North American grid in 2013-2014 [8]

However, a battery has an estimated amount of throughput over its lifetime which is given by the manufacturer. Usually, it is considered that the battery has reached

end-of-life when the actual throughput reaches the estimated value. The amount of the lifetime throughput is obtained by various test methods under standard conditions, but these conditions are usually not achievable in real-time operation. The operating conditions of a battery are typically more severe than those used in the standard tests of cycling and float lifetime. There are different stress factors to consider in real-time operation such as partial state of charge (SoC) cycling, the time since the last full charge, incomplete or rare full charging etc.. Due to these stress factors, there is a deviation from the standard conditions introducing weight factors that continuously multiply with the actual throughput called weighted throughput. The high value of weighting factors lead to the higher amount of throughput and reduce the battery lifetime drastically.

1.2 Previous Work

This section begins with a brief review of different optimization techniques. Afterwards, EMSs with different batteries are presented. Finally, the operating condition of batteries and different weight factors that model the battery throughput in EMSs are presented.

1.2.1 Optimization Techniques Applied in EMS

Several methods have already been developed to solve optimization problems in EMSs. A particle swarm optimization (multiobjective) technique was used in an EMS to obtain minimum operational cost [11] considering the distributed energy generators cost. The objective function was the weighted sum of different objectives. A weight determines the priority of that particular objective to achieve the overall goal. The authors considered random values of the weights.

A multi-objective optimization model has been proposed for a microgrid EMS [12]. A fast non-dominated NSGA-II algorithm was selected to solve the optimization problem under different circumstances. An optimal solution set was obtained through a multi-objectives optimization problem although single-objective optimization problem was solved at a time. The authors didn't considered the importance for any particular objective.

A multi-objective optimization technique using Genetic Algorithm (GA) is presented in [13] to minimize the energy generation cost and maximize the storage device lifetime in microgrids. The authors considered equal importance for the both the objectives. In [14], a Fuzzy mathematics based multi-objective optimization technique is introduced without having weighted objective function.

Therefore, multiobjective optimizations were considered in the literatures using different algorithms but there was no effort to determine the optimal value of weights. An optimal point could be found by changing the values of the weights in objective function to achieve the final goal with optimizing the individual objective.

1.2.2 Microgrids with Different Energy Storage Systems

A study in [15], used a model to compare lead acid (PbA) and Aqueous Hybrid Ion (AHI) batteries using in realistic microgrid by using HOMER software. The study suggested that a AHI-based microgrid system utilized 10-30% more PV power and provided 10% more cost-effective solution even though initial cost is higher than PbA-based systems; however, the authors concluded that a AHI-based system is a more reliable option for a system which required frequent charging and discharging. It was also

found that initial levelized cost of electricity (LCOE) is the most important factor to evaluate different energy storage technologies in terms of operational costs of the systems. The authors only compared PbA and AHI batteries.

A feasibility study on pumped hydro and battery storage (considered 50% and 100% DoD) for a renewable energy system in an island was conducted in [16], where the authors considered different scenarios and analyzed the corresponding life cycle cost. It was found that batteries with low allocable DoD lead to high life cycle cost. However, a pumped hydro alone system offered the best cost solution, although the authors didn't consider the maintenance cost of pumped hydro and in remote microgrids frequent maintenance is uneconomical. There was no effort to study the feasibility of other storage devices for remote microgrid.

Rebecca et. al. [17], presented a comparative techno-economic analysis of lead acid, and and Li-ion batteries for microgrid uses. The study suggested that the discount rate of storage devices together with levelized cost of electricity (LCOE) plays a crucial role in achieving the most effective solution. Although, the authors concluded that the low cost with high energy density Li-ion battery offers the best solution, there was no effort of optimal use of the battery along with prolonging the lifetime and not even any consideration of the battery float life cost. However, the authors only consider two types of batteries.

However, the literature compares and analyzes only two different types of energy storage systems. The literature lacks a comparative economical analysis of a range of storage devices including generator fuel consumption and storage device lifetime.

1.2.3 Battery Weighted Ah-throughput Model

A weighted Ah throughput model was developed by Schiffer et al. in 2007 [18], predicts the lifetime of a lead acid battery. In the model, the authors considered different aging parameters such as corrosion, acid stratification, sulphation, gassing, discharge current, SoC, consecutive charging time, and temperature. To calculate the actual throughput from the battery, different weighting factors were multiplied with calculated throughput. The same battery model was implemented by Rodolfo et al. in 2013 [19] and compared with other models. The Schiffer AH model was found to be the most accurate to demonstrate a battery. To design a control system of battery storage and wind energy system in [20], SoC weighting factor from Schiffer AH model was considered in the battery model.

In [21], a battery charging/discharging scheme was proposed to avoid detrimental operation of battery so that the battery lifetime can increase. In the battery model, the authors considered SoC weighting factor to determine the actual throughput from the battery although for the sake of simplicity, the impact of SoC and corresponding factor were considered and the rest were ignored. Moreover, the authors included the Schiffer Ah model in the real-time energy market rather than the remote microgrids EMS.

Chalise et al. [22] developed a power management strategy for remote microgrids considering lead acid battery lifetime. To model the battery, the Schiffer Ah model was considered and for the sake of simplicity only SoC weighting factor was included. The authors proposed a weekly cycling strategy to reduce the SoC weighting factor. But, the authors did not consider the weight factor in the objective function of the EMS.

In summary, most of the current literature focused on the analysis of different weight factors in the battery model but did not incorporate in the EMS of remote microgrids. Only one article considered SoC weight factor in the remote microgrids EMS for analyzing the impact on the battery lifetime deterioration, although did not incorporate in the objective function.

1.3 Motivation

Motivation of this thesis is the need of cost effective energy storage technology for remote microgrids EMS to obtain minimum fuel operational cost and fuel consumption with high life span and a battery cycling strategy to mitigate faster battery degradation due to irregular operating condition.

1.4 Objectives

The objectives of this thesis are:

1. Analyze the feasibility of using PbA, Li-ion, AHI batteries and ultracapacitor in remote microgrids EMS.

2. Incorporate Schiffer Ah-throughput model in the objective function of the EMS to analyze the effect of SoC weight factor in faster battery degradation and investigate different battery cycling strategies to mitigate that effect.

1.5 Contributions

There are two different contributions of this thesis. The first contribution is the feasibility study of different energy storage technologies to use in the remote microgrids EMS. The second contribution is the analysis of different battery cycling strategies to reduce the value of SoC weight factor in order to protect the battery from faster

degradation. In the analysis, consideration was given to low minimum operational cost and generators fuel consumption.

1.6 Thesis Outline

This thesis has been organized as follows: Chapter 2 presents the different components of a microgrid and a brief description of different energy storage technologies available in the market and the comprehensive illustration of the Schiffer Ah-throughput model. Chapter 3 deals with the description and modelling of the components in a microgrid and modified EMS. Results and corresponding analysis are presented in Chapter 4, followed by conclusions and future works.

CHAPTER 2 THEORY

This chapter presents the theory related to this thesis. Section 2.1 describes the microgrids and its classification. Section 2.2 presents the operation of a remote microgrid energy management system (EMS). The EMS describes the day ahead scheduling and real time dispatch of distributed energy resources. The operating principle and characteristics of diesel generators, photovoltaic systems and energy storage systems are presented in Section 2.3. Section 2.4 demonstrates battery weighted throughput model which was included in this thesis to consider the different operating conditions of battery. Further, Section 2.4.1 describes the Schiffer weighted Ah-throughput model.

2.1 Microgrids

Microgrids are small and integrated energy systems capable of managing interconnected loads and distributed energy sources intelligently and maintain stable operation within a defined boundary either in independently or parallel with utility grid [23]. A microgrid can ensure the optimal power quality, reliability, and economical benefits when it is running in grid connected mode or off-grid mode. It can be powered by distributed energy sources (PV, wind and so on), microturbines, diesel generators, energy storage system that supply to different kind of loads which are monitored by intelligent control system.

In recent research, there are five major categories of microgrid were identified [24].

(1) Institutional and Campus Microgrids

(2) Commercial and Industrial Microgrids

(3) Military Microgrids

(4) Community and Utility Microgrids

(5) Remote Microgrids

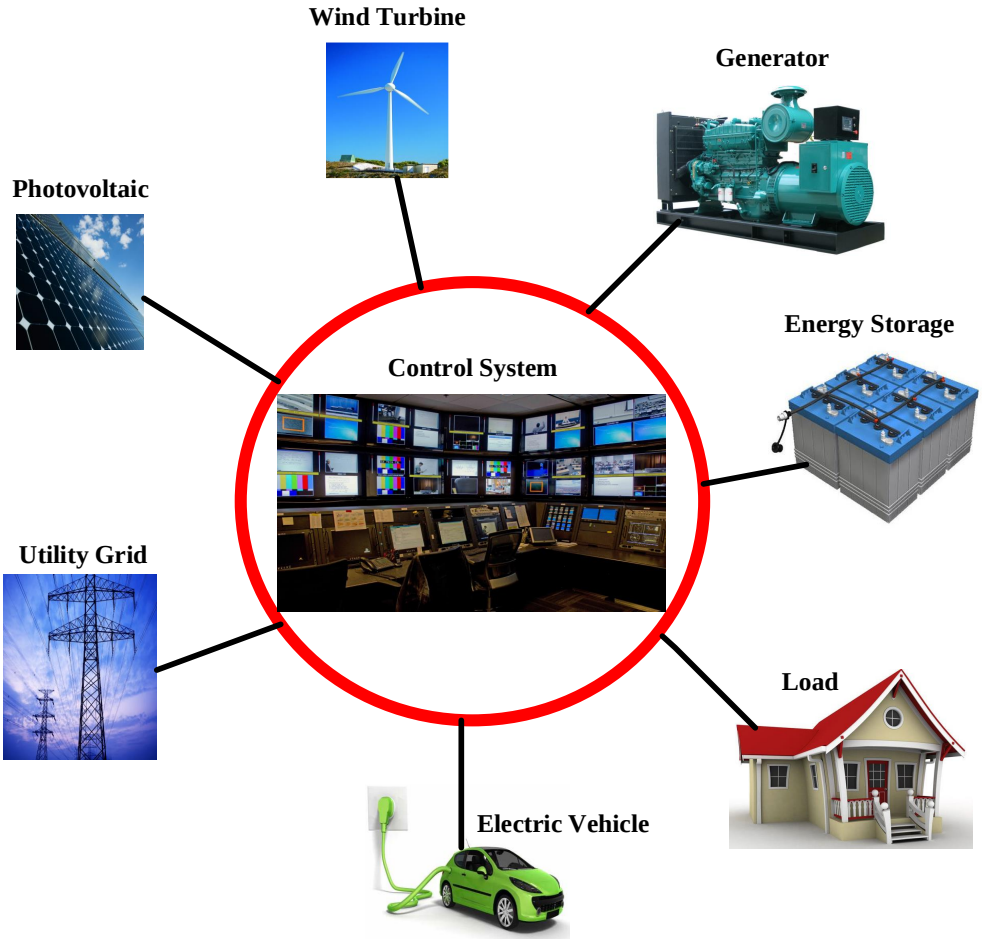

Figure 2.1. A simple microgrid

2.1.1 Remote Microgrids

Remote microgrids are disconnected from the utility grid due to geographical location. The main idea of remote microgrids is to power the rural communities where the population is small. Rural communities mainly use electricity for their household work, irrigation, and commercial loads. Single or multiple owner can participate to develop such system and for being small in size it is more simpler than the other systems. In such

system, customers have to pay high electricity price due to high transportation cost of generators fuel. Moreover, maintenance and replacement of the components (specially the storage device) are important issues in remote microgrids to operate the system cost effectively by improving fuel efficiency and energy storage lifetime.

2.2 Remote Microgrids EMS

EMS is the core part of remote microgrids that efficiently coordinates the distributed energy energy resources (DERs) of different capacities. Typically, there are two distinctive layers in the microgrids EMS to schedule and dispatch the distributed energy resources (Figure 2.2).

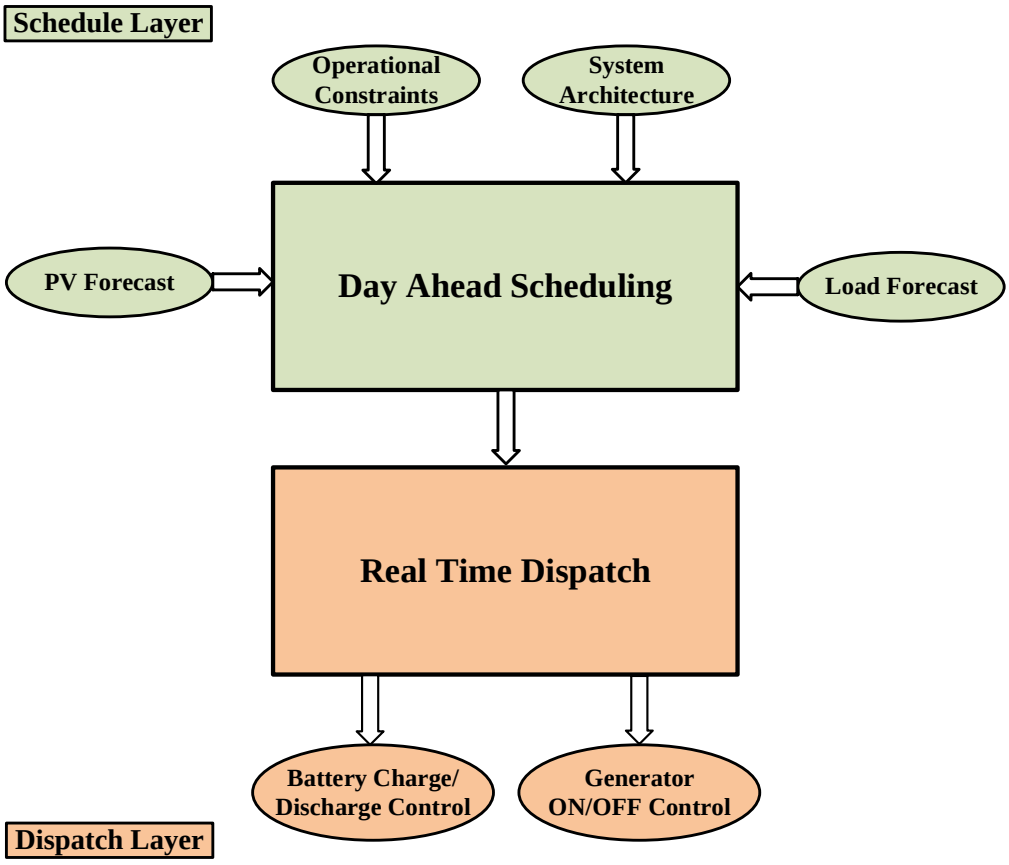

Figure 2.2. Two layers EMS in remote microgrids

2.2.1 Day Ahead Scheduling

Scheduling is the process of allocating the DERs for operation over a horizon of time, and it is performed by the master controller considering the economic benefits. It is required to find the optimal power set point of DERs in a time ahead system. Typically, a day ahead approach is used to perform the DERs scheduling. However, there are forecasting and optimization tools in the schedule layer. Forecasting tool forecasts the renewable energy and the load demand in different periods of a day. Forecasting is used to utilize the maximum renewable energy, and reduces the required reserve. Then the calculated net load (forecasted load-PV) information is transferred to the optimization tool. Optimization provides the most economic scheduling result satisfying all the constraints over a scheduling horizon. According to the system operational constraints, the optimization tool performs the economical dispatch considering different objectives of the system such as low operational cost, generator fuel consumption, and high battery life time. The optimization method can be deterministic or stochastic in nature. There are different types optimization are analyzed in [11]-[12]. A goal programming approach can be used to achieve multi-objective optimization [25]. After performing the optimization, the dispatching signal send to the dispatch layer.

2.2.2 Real Time Dispatch

Real time dispatch layer receives the dispatching signals from the scheduling layer with power set point of generators and battery, and dispatch accordingly. The dispatching process is controlled by the master controller, and the dispatching signals transmit through the advanced information communication technology infrastructure (ICT). To ensure the

smooth operation, dispatch layer should not lose the effectiveness of the schedule layer. Real time dispatch ensures power system reliability and power quality. In addition, any deviation from the schedule layer is compensated in the dispatch layer. However, dispatch efficiency can be increased by using consumer based demand side management system (DSM) scheme [26].

2.3 Remote Microgrid Components

A remote microgrid is typically consists of diesel generators, energy storage systems, and renewable energy sources (only PV system was considered in this thesis).

2.3.1 Diesel Generators

A diesel generator is a combination of diesel engine and synchronous generator which converts mechanical power into electrical. The diesel engine provides the external mechanical energy which is converted into electrical output by a synchronous generator. The speed of diesel generators are controlled by a governor to control the output frequency. The governor mainly control the fuel injection that regulates the speed of the rotor. An automatic voltage regulator (AVR) is used to maintain the generator output voltage within a certain limit depending upon the loads by controlling its field excitation current. AVR senses the voltage by using a power-generating coil; compare to a reference and then the error signal is used to adjust the field current (Figure 2.3).

The fuel consumption of diesel generators can be expressed in terms of fuel consumption rate and fuel efficiency. The fuel consumption rate is the amount of fuel consumed by the generator in an hour to produce a certain amount of power output. The manufacturer usually provides the data related to fuel consumption rate which can be

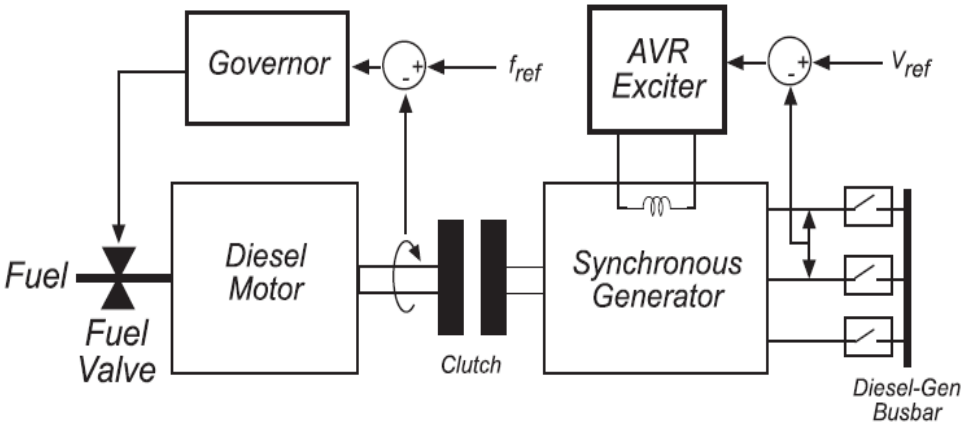

Figure 2.3. Block diagram of a diesel generator [27]

expressed in a polynomial relation as given in Equation 2.1.

$$F = aP_g^2 + bP_g + c \tag{2.1}$$

where, a, b and c: generator fuel curve coefficients; P_g: generator output power. Higher value of P_g leads towards the high fuel efficiency.

The fuel efficiency of a diesel generator can be expressed by using Equation 2.2 [28],

$$\eta_g = \frac{3600 \times P_g}{\rho_f \times (aP_g^2 + bP_g + c) \times LHV_f} \tag{2.2}$$

where, LHV_f: lower heating value of the fuel (MJ/Kg), ρ_f: fuel density in Kg/m^3. For diesel generators, LHV_f=43.2 MJ/Kg and ρ_f=820 Kg/m^3 [28].

By using Equation 2.1 and 2.2, the fuel consumption characteristics of a 75 kW diesel generator can be obtained as in Figure 2.4. The total operating region of a diesel generator can be divided into three zones based on the output power (% of rated power)

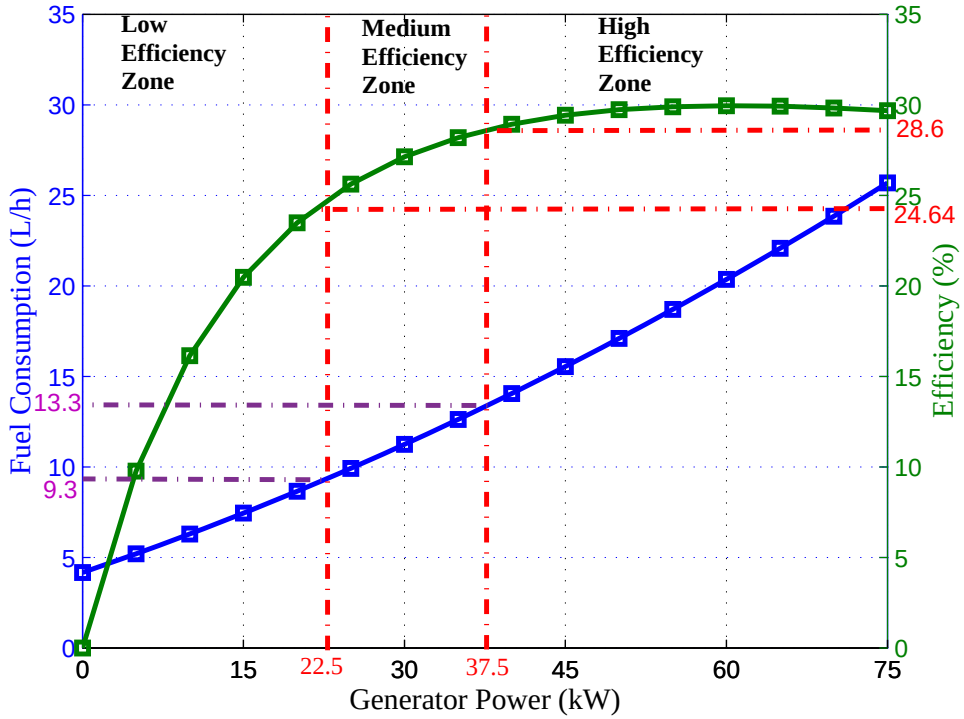

Figure 2.4. 75 kW diesel generator fuel efficiency characteristics

such as low ($< 30\%$), medium ($30 - 50\%$) and high ($> 50\%$) efficiency zone [28]. High fuel efficiency can be obtained by operating the generator near to rated load. While the diesel generator is operating in low load condition ($P_g < 22.5$ kW), the efficiency can be maximum 24.64% (Figure 2.4). At half load condition, fuel efficiency is increased by 4% and the maximum efficiency can be achieved at near to full load. It is economical to operate the diesel generator at 80-90% of rated power. Furthermore, the manufacturer also suggests not to operate bellow 30% of rated load.

2.3.2 Photovoltaic System

A photovoltaic (PV) system is a DC power generation system that converts sunlight into electrical energy using p-n semiconductors that exhibits PV characteristics. The materials with PV effect called solar cell, absorbs photon from light and release electrons

that results the electric current in the system. The equivalent circuit of a solar cell can be presented by an ideal current source with parallel diode and resistance as in Figure 2.5 [29]. The current source represent the current that is generated from the photons.

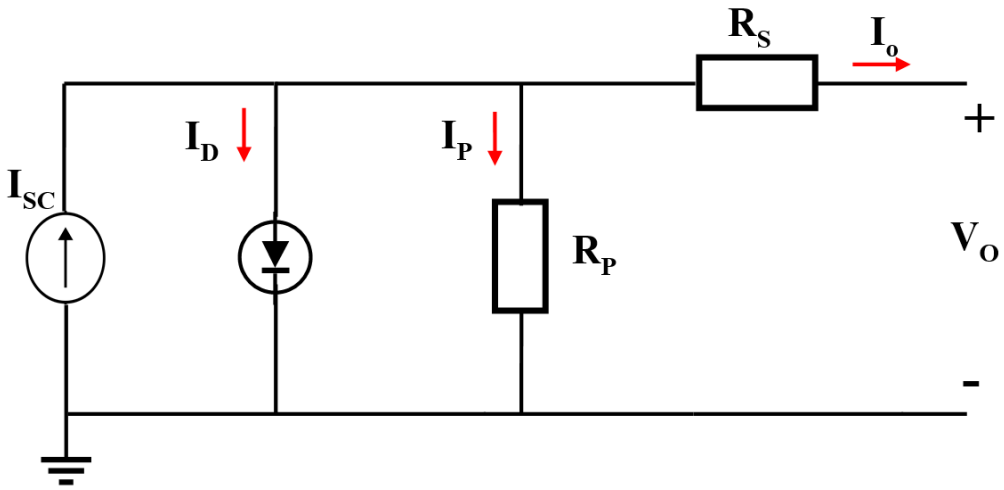

Figure 2.5. Equivalent solar cell circuit [30]

The output current power of a solar cell can be written as

$$I_o = I_{SC} - I_D - I_P \tag{2.3}$$

$$P = VI_o \tag{2.4}$$

where, I_{SC}: photon generated current (A); I_o: solar cell current, and I_D: diode current which can by given by Equation 2.5 [29].

$$I_D = I_d[exp(\frac{q(V_o + I_o R_S)}{nKT}) - 1] \tag{2.5}$$

Now, Equation 2.3 can be written as

$$I_o = I_{SC} - I_d[exp(\frac{q(V_o + I_o R_S)}{nKT}) - 1] - \frac{V_o + I_o R_S}{R_P} \tag{2.6}$$

where, V_o: output voltage (V) or, open circuit voltage, V_{oc}; I_d: diode saturation current (A); q: one electron charge ($1.6 \times 10^{-19}\ C$); T: solar cell temperature (K); K: Boltzmann constant (1.38×10^{-23}); R_S: solar cell series resistance (Ω); R_P: solar cell shunt resistance (Ω) and n: ideality factor ($1 < n < 2$) [31].

The electrical output of a solar cell is proportional to the amount of solar irradiation (W/m^{-2}). Power vs voltage plot of a solar cell is presented in Figure 2.6.

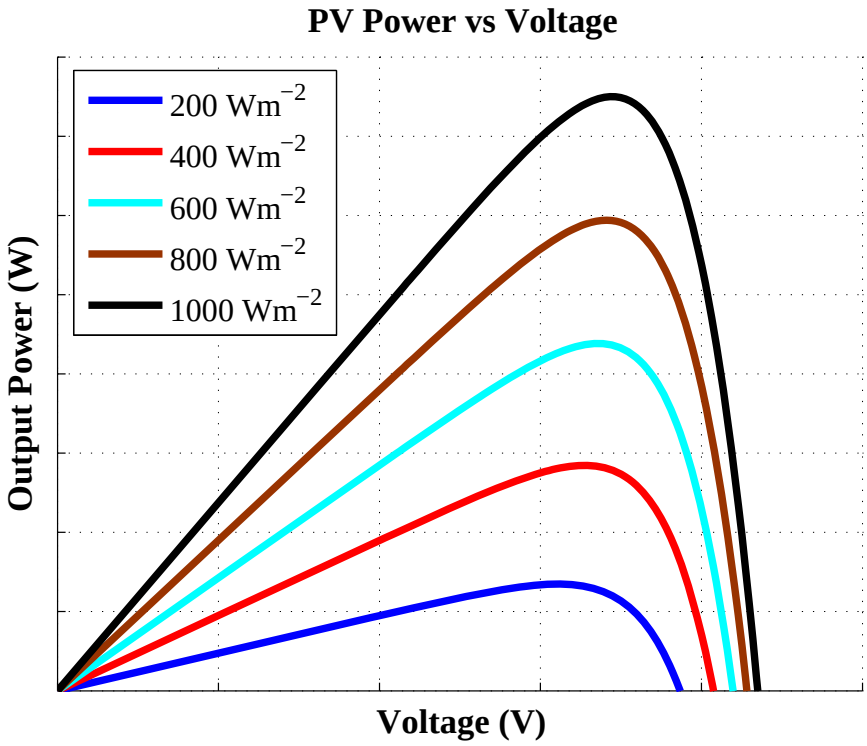

Figure 2.6. Power vs voltage plot of a solar panel for different solar irradiance (Wm^{-2})

The maximum power from a solar panel can be obtained by operating the solar cell at I_{MPP} and V_{MPP} where the panel power is maximum (Figure 2.7). However, a maximum power point tracker (MPPT) can be used to extract the maximum power from a solar

panel.

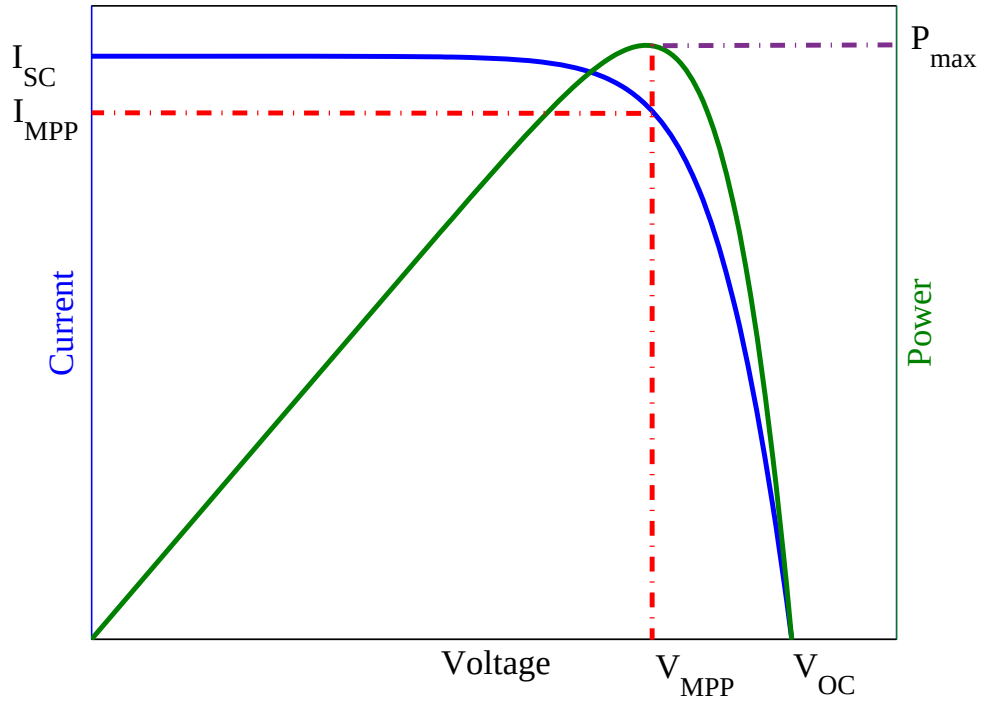

Figure 2.7. Maximum power point operation of a solar panel

The maximum power output from a PV system can be expressed as in Equation 2.7, in terms of nominal capacity (PV_n), solar irradiance (G), STC solar irradiance (G_{STC}) which is 1000 Wm^{-2} at 25 ^oC, and PV derating factor f_{df} [32].

$$P_{PV}(t) = f_{df} PV_n \frac{G(t)}{G_{STC}} \tag{2.7}$$

2.3.3 Energy Storage System

An energy storage system is a significant component of remote microgrids. By balancing the power generation and demand, the ESS improves the system reliability and efficiency. Moreover, in microgrids EMS, ESS reduces the use of dump loads and PV power curtailment to operate the diesel generators in the high efficiency zone. There are

various types of electrical energy storage systems which can be classified into different categories (Figure 2.8) [33].

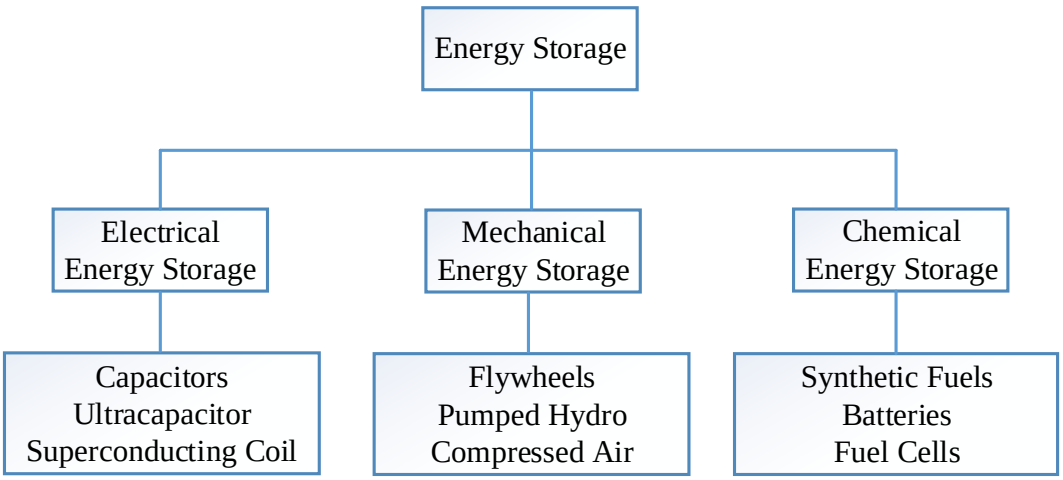

Figure 2.8. Different energy storage technologies

2.3.3.1 Lead Acid Battery

Lead acid (PbA) batteries are the oldest and most established rechargeable energy storage technology that are being used in the present microgrids. Lower cost compared to the other battery technologies wide speareds its adoption; however, slow response rate, short life cycle, and depth of discharge (DoD) are its major drawbacks. Depending on the configuration of electrodes, the operation of lead acid batteries are categorized into shallow discharge and deep-discharge mode. Shallow discharge batteries are suitable for automobile applications while deep-discharge lead acid batteries are mainly applicable for small cycle renewable energy systems [34].

2.3.3.2 Lithium-ion Battery

Currently, lithium-ion (Li-ion) batteries are the prominent storage technology for PV systems and portable and mobile applications (e.g. laptop, mobile phone, electric

Table 2.1. PbA batteries [35]

Efficiency (%)	70-90
Life cycle (cycles)	500-2000
Float life (years)	5-15
Specific energy (Wh/kg)	30-50
Initial cost ($/kWh)	100-600
Operation and maintenance cost ($/kW-year)	12-30

vehicle) due to its high flexibility. Compared to the other technologies, Li-ion batteries have high efficiency, energy and power density, life cycle, allowable DoD, and faster response rate; however, its initial ivestment cost is high and requires sophisticated charge management and control system.

Table 2.2. Li-ion batteries [36]-[37]

Efficiency (%)	85-98
Life cycle (cycles)	1,000-10,000
Float life (years)	5-15
Specific energy (Wh/kg)	75-200
Initial cost ($/kWh)	500-2,500
Operation and maintenance cost ($/kW-year)	12-30

There are different kind of Li-ion batteries such as

- Lithium Cobalt Oxide ($LiCoO_2$)
- Lithium Manganese Oxide ($LiMn_2O_4$)
- Lithium Iron Phosphate ($LiFePO_4$)
- Lithium Nickel Manganese Cobalt Oxide ($LiNiMnCoO_2$)
- Lithium Nickel Cobalt Aluminum Oxide ($LiNiCoAlO_2$)
- Lithium Titanate ($Li_4Ti_5O_{12}$)

Among all the Li-ion batteries, lithium iron phosphate ($LiFePO_4$) is an emerging storage technology with high life cycle, faster response rate, and considerably higher current rating, although the initial cost is very high.

2.3.3.3 Ultracapacitor

Ultracapacitor(UC), also known as supercapacitor, is the energy storage technology that stores energy in form of electrical charge between two metal plates separated by dielectric materials. UCs have high power density, efficiency, and high life cycle. High initial cost is a major drawback to use in the large scale power systems. UCs are highly appropriate for such a systems that requires high power density particularly hybrid electric vehicle. In the USA, there are a number of UC energy storage systems installed in microgrids [38]. Japan has also been analyzed the performance of UC in microgrids specially for voltage sag compensation and power smoothing [39]. UC and batteries (specially the PbA battery) can form a hybrid energy storage system that may optimize the power and energy density of the storage system.

Table 2.3. Ultracapacitor [35]

Efficiency (%)	85-98
Life cycle (cycles)	10^5-10^6
Float life (years)	4-12
Specific energy (Wh/kg)	5-30
Initial cost ($/kWh)	300-20,000
Operation and maintenance cost ($/kW-year)	N/A

The operation of battery/ultracapacitor (UC) depends on the present state of charge (SoC) to dispatch the battery/UC for charging and discharging correspondingly. During the charging and discharging period, the next hour SoC of battery/UC (Equation (2.8) and (2.9)) depends on the present hour SoC, charging/discharging power, battery/UC capacity,

charging/discharging efficiency, and the time duration of charging/discharging.

$$SoC_{bat}(t+1) = SoC_{bat}(t) + \frac{\eta P_b(t)\Delta t}{C_b} \tag{2.8}$$

$$SoC_{UC}(t+1) = SoC_{UC}(t) + \frac{\eta P_{UC}(t)\Delta t}{C_{UC}} \tag{2.9}$$

and,

$$\eta = \begin{pmatrix} \eta_{ch}, charging \\ 1/\eta_{disch}, discharging \end{pmatrix}$$

where, t: present time; $SoC(t)$: the present hour SoC; $SoC(t+1)$: the next hour SoC; $P_b(t)$: present hour battery charging/discharging power at t, (kW); $P_{UC}(t)$: present hour UC charging/discharging power at t, (kW); C_b: battery capacity, (kWh); C_{UC}: UC capacity, (kWh); Δt: charging/discharging duration; η_{ch}: charging efficiency; η_{disch}: discharging efficiency.

2.4 Weighted Throughput Modelling

Generally, the throughput is considered as the amount of discharging energy from a ESS under standard conditions but these are not achievable in real time operation. There is a virtual increase (or decrease) in the standard test throughput due to the different physical and chemical stress factors [40]. Major stress factors in operation of a lead acid battery are described in [41]-[42] which may cause deviation from the standard conditions. Considering all those factors, equivalent weighted throughput can be determined to represent the actual operating conditions [19]. Moreover, the expected lifetime of the ESS can be estimated from the weighted throughput model.

2.4.1 The Schiffer Weighted Ah-throughput Model

A weighted Ah-throughput model was developed by Schiffer et. al. considering different stress factors in the operating conditions during the battery operation [18]. This model is valid only for lead acid battery and assume that the operating conditions are more severe than the standard test conditions. The major stress factors in this model are minimum operating SoC, time between full charge, discharging current, incomplete or rare full charging, and operating temperature. Considering the aforementioned stress factors, two weight factors were introduced in the Schiffer model that should be multiplied with the actual throughput to get the weighted throughput from the battery. The two weight factors are

(1) SoC weight factor, (W_{SoC})

(2) Acid weight factor, (W_{Acid})

2.4.1.1 SoC Weight Factor, W_{SoC}

The SoC weight factor, W_{SoC} takes into account the impact of SoC and discharge current on the battery operation. Cycling operation at lower values of SoC over a long period of time since the last full charge introduces mechanical stress, consequently affects the battery lifetime. Additionally, the discharge current affect the growth of sulphate crystal called sulfation, and degrade the battery capacity. The first cycle of discharging current of a fully charged battery mainly influenced the sulfation. Higher the value of the discharge current results in a high number of small sulphate crystals. The impact of operating SoC and discharging current modeled by the factor W_{SoC} (Equation 2.10).

$$W_{SoC}(t) = 1 + (C_{SoC,0} + C_{SoC,min} \times (1 - SoC_{min}(t)|_{t_o}^{t}) \times W(I, N_{bc}) \times (t - t_o)) \quad (2.10)$$

where, $C_{SoC,0}$ and $C_{SoC,min}$ are the constant slope for SoC factor and impact of the minimum SoC on the SoC factor respectively at SoC=0. In Equation 2.10, the current factor, $W_I(I, N_{bc})$ is the combination of sulfation effect and bad charge/partial full charge (charging at $0.9 <$ SoC < 1) effect which can be calculated by Equation 2.11

$$W_I(I, N_{bc}) = \sqrt{\frac{I_{10}}{I_f(t)}} \times \sqrt[3]{exp(\frac{N_{bc}(t)}{3.6})} \quad (2.11)$$

I_{10} is the 10 hour current which can be calculated as, $I_10 = C_{10}/10$ where, C_{10} is the battery nominal capacity. $I_f(t)$ is the discharging current at first cycle immediate after one full charge. In Equation (2.11), N_{bc} is the number of bad charges when the battery is in charging condition at SoC > 0.9, and charging at SoC < 0.9 will not account the bad charges. The number of bad charges is reset to zero when the battery is fully charged. N_{bc} is calculated when the operating SoC is between 0.9 to 1, and it is in charging condition (Equation 2.12).

$$N_{bc}(t + \Delta t) = N_{bc}(t) + \frac{0.0025 - [0.95 - SoC(t + \Delta t)]^2}{0.0025} \quad (2.12)$$

The coefficient $C_{SoC,0}$ and $C_{SoC,min}$ are constant parameters adopted from [18] and the value of I_{10} can be determined from the manufacturer sheet. The variables $SoC_{min}(t)|_{t_o}^{t}$, Δt_{SoC}, and $I_f(t)$ are schematically illustrated in Figure 2.9. Figure 2.9 (a) (red

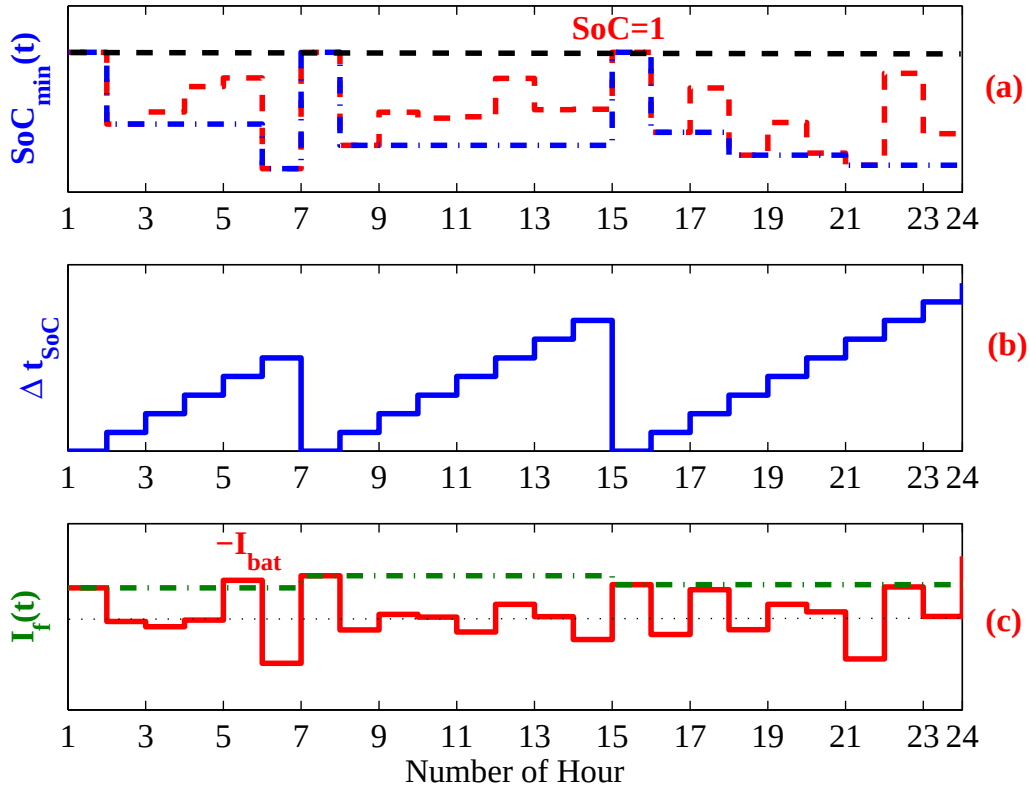

Figure 2.9. Schematic illustration of the (a) sample hourly initial SoC profile throughout a day, and minimum SoC from the last full charge, $SoC_{min}(t)|_{t_o}^{t}$ (b) time from the ast full charge, Δt_{SoC} and (c) current at first cycle of discharge after a full charge, I_f

dash line) shows a hourly initial SoC profile of a battery over 24 hours of a day, and initially, the battery is fully charged (SoC=1). Afterwards, the battery gets full charge at hour 7 and 15. There are a number charging and discharging cycle in the rest of the hours.

$SoC_{min}(t)|_{t_o}^{t}$ is the minimum SoC since the last full charge which is presented in the Figure 2.9 (a) (blue dash line). It can be seen that at hour 2, battery SoC decreases as it is discharging, and thereafter, it is being charged (SoC increases) till hour 5. So that, the value of SoC_{min} from hour 2-5 is equal to the SoC at hour 2 as it is the minimum value since the hour 1. Similarly, the value of SoC_{min} can be determined at hour 6, from hour 8-14, 16-17, 18-20 and 21-24. The value of SoC and SoC_{min} is 1 when the battery is fully

charged.

$\Delta t_{SoC} = t - t_o$, where t is the present time and t_o is the time of the last full charge. Since the time difference from the last full charge to present time increases, the value of Δt_{SoC} increases from hour 2-6, 8-14, 16-24 (Figure 2.9 (b)).

I_f is the current at the beginning of the discharge after a full charge which can be obtained at the beginning of hour 1, 7 and 15 (Figure 2.9 (c)) (green dash line).

2.4.1.2 Acid Weight Factor, W_{Acid}

The acid weight factor, W_{Acid} mainly takes into account the acid stratification during battery operation that results in a gradient of the acid concentration. The main factors that influence the W_A are the minimum SoC since the last full charge ($SoC_{min}(t)|_{t_o}^{t}$), gassing current, temperature, and battery current (charging and discharging). Lower battery current and minimum SoC since the last full charge have the higher impact on W_A. The total impact of W_A can be described by

$$W_A(t) = 1 + W_S(t)\sqrt{\frac{I_{10}}{|I_{bat}|}} \tag{2.13}$$

where, W_S is the acid stratification factor which is composed of two factors that describes the impact of acid stratification increase and decrease.

$$W_S(t + \Delta t) = W_S(t) + (W_{in}(t) - W_{de}(t))\Delta t \tag{2.14}$$

The factor W_{in} incorporates the effect of the discharge current and $SoC_{min}(t)|_{t_o}^{t}$ which can be calculated as

$$W_{in}(t) = C_{in} \times (1 - SoC_{min}(t)|_{t_o}^{t}) \times exp(-3W_S(t) \times \frac{I_{dis}(t)}{I_{10}}) \quad (2.15)$$

The effect of acid stratification is reduced by diffusion and gassing of acid. Therefore, the total factor for the decrease of acid stratification is

$$W_{de}(t) = W_{de,gassing} + W_{de,diffusion} \quad (2.16)$$

The factor for the decrease of acid stratification, $W_{de,gassing}$ can be calculated as

$$W_{de,gassing}(t) = C_{de} \cdot \sqrt{\frac{100Ah}{C_N}} \times \frac{I_{gas,0}(t)}{I_{gas,ini}} \times exp(C_v(V_{cell} - Vref) + C_T(T - T_{gas,0})) \quad (2.17)$$

The decrease of acid stratification due to diffusion is given by

$$W_{de,diffusion}(t) = \frac{8D}{z^2} \cdot W_S(t) \cdot 2^{(t-20^\circ C)/10K} \quad (2.18)$$

In the Equation 2.16-2.18, C_{in} and C_{de} are the factors for increase and decrease of acid stratification respectively; $I_{gas,0}(t)$ and $I_{gas,ini}$ are the normalized and initial normalized gassing current; T is the temperature; V_{cell} is the cell voltage; V_{ref} is the reference voltage; D is the effective diffusion constant; z is the height of the electrodes. Those parameters can be adopted from [18]. C_N is the nominal capacity which can be obtained from the data sheet.

CHAPTER 3 PROCEDURE

Chapter 3 describes detailed procedure of this thesis that were followed to complete the following tasks.

Task 1: Analyze the economical prospectives of different storage devices for remote microgrids energy management system (EMS).

Task 2: Incorporate the Schiffer weighted Ah-throughput model in the objective function and analyze the battery cycling strategies.

Section 3.1 describes a developed remote microgrid benchmark which was considered in this thesis. Including monthly load and PV (photovoltaic) profile, the cost modeling of some components of that benchmark (diesel generator and storage device cost modeling are required in this study) are presented in the Section 3.2. To complete the Task 1, a mathematical model of the EMS using deterministic approach is defined in the Section 3.3. The EMS algorithm is described with an objective function and a set of constraints. Section 3.4 describes the procedures to incorporate the Schiffer model in the EMS (Task 2). Furthermore, a modified state of charge (SoC) weight factor and weighted battery throughput model are presented in the Section 3.4.1 and 3.4.2 respectively. Section 3.5 demonstrates the case studies of Task 2 to find the cost effective battery charging strategy to minimize the value of SoC weight factor.

3.1 Remote Microgrid Benchmark

A microgrid benchmark is described in Figure 3.1, which was developed by Santosh et. al. [22]. This microgrid consists of 30 kW photovoltaic panels, and two KOHLER generators of 30 kW (model: 30REOZJC) and 75 kW (model: KT75). The diesel cost of

the generators was considered $8.00 per gallon based on remote community electric utility [43]. Generators are limited to supply minimum power of 30% of their rated capacity. Furthermore, a battery energy storage system exists in the system to balance the power supply and demand. The battery bank was seized to supply the four hour average load of the system. The peak and average load of the system are about 64 kW and 25 kW respectively, and the most of the loads are residential in type. In order to ensure optimum operation, the EMS forecasts the load and PV power, and afterwards, schedule and dispatch the DERs. However, the EMS communicate with the system components through the local controllers.

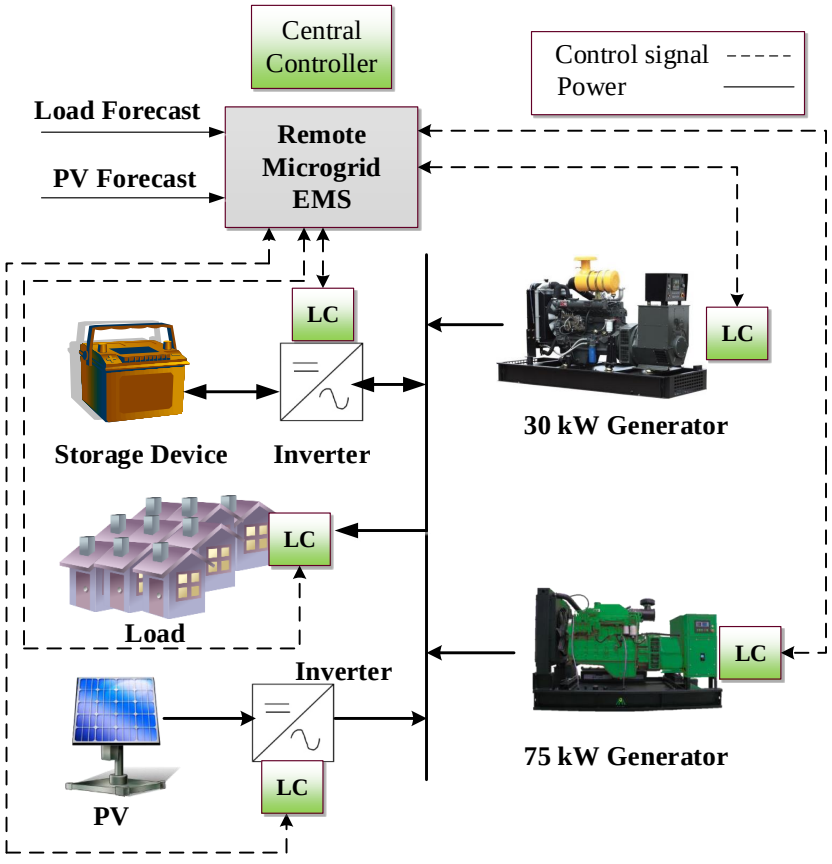

Figure 3.1. Microgrid benchmark [22]

The EMS has two different functions: 24 hours (day ahead) scheduling and real time dispatch of the generators and the energy storage devices. A day ahead scheduling technique is used to obtain the minimum fuel consumption, to obtain the minimum operational cost, and to prolong the battery lifetime whereas real time dispatch ensures the system reliability and power quality. In the microgrids EMS, the operational cost of the power electronics converters and PV panels were considered constant.

3.2 Mathematical Model of the Components

3.2.1 Loads

In the microgrid, the loads are classified into residential, critical, and non-critical. The critical loads are mainly the commercial loads such as health clinic, and the non-critical loads are such as water pumps and water heater. In this study, an hour based yearly load profile was collected from Nemiah Valley microgrid [44]. Figure 3.2 shows the monthly load information whereas the yearly maximum, minimum and average loads are about 64 kW, 3 kW and 25 kW accordingly. In this load profile, the peak to average load ratio is 2.56. The average load is comparatively high in the late autumn to winter (November to April) and low in the summer season. The peak and average load are also higher in the winter season than that in the summer. Figure (3.3) illustrates the daily load data over 24 hours for four different days of summer (9^{th} July and 12^{th} August) and winter (19^{th} December and 10^{th} January) season. The peak to average load ratio is slightly higher in the summer season. This ratio is 1.62, 2.01, 1.28 and 1.35 on 9^{th} July, 12^{th} August, 19^{th} December and 10^{th} January respectively. The peak and average load both are the highest on 10^{th} January (56.45 kW and 41.84 kW accordingly).

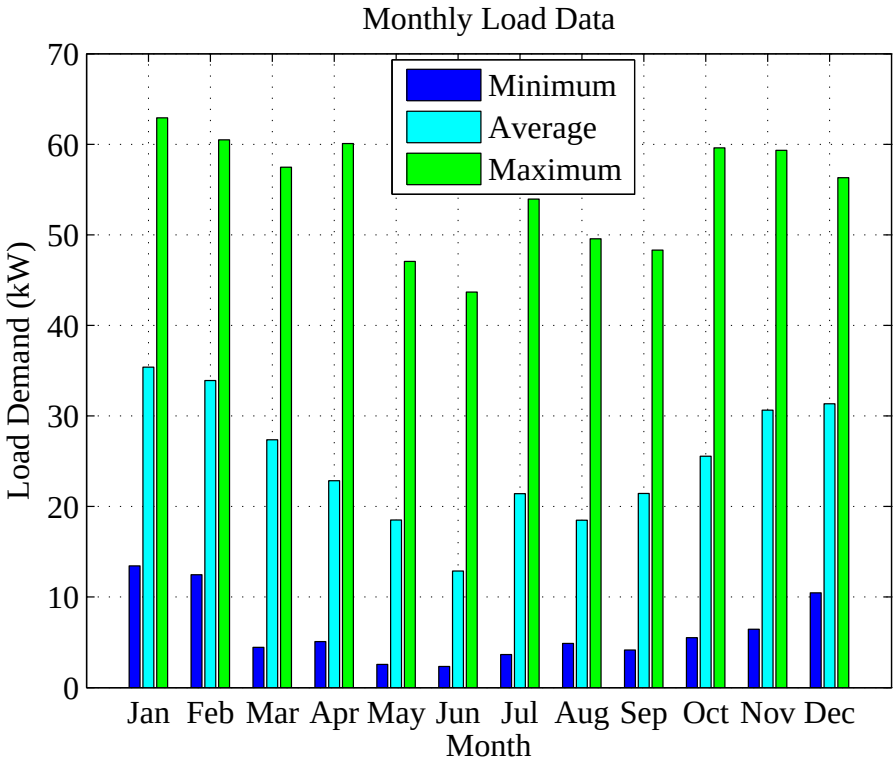

Figure 3.2. Monthly load data throughout a year

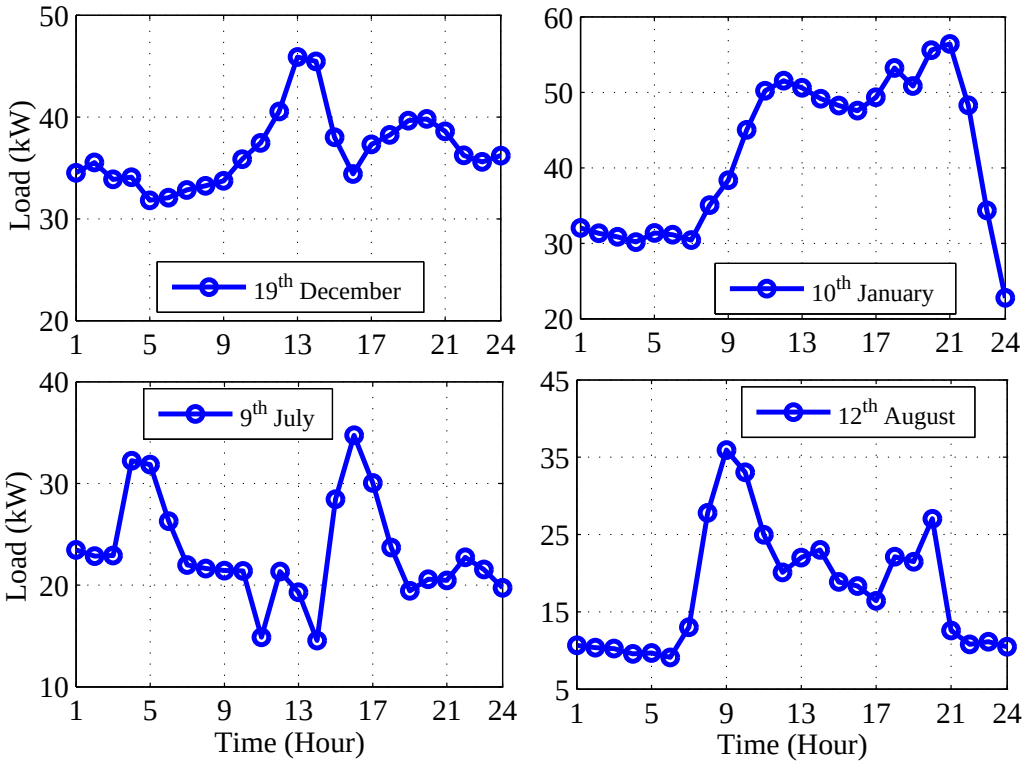

Figure 3.3. Load data in four different days

3.2.2 Photovoltaic Generation

The yearly photovoltaic (PV) profile is presented in the Figure 3.4 which was given in hour basis [44]. The average and maximum PV power were about 5 kW and 30 kW respectively. Compared to the winter season, the average PV power generation is high during the summer due to the availability of sun over a longer period of time. Figure 3.5 shows the PV profile of four different days of the winter and summer season. Typically, peak PV power is obtained at noon (12.00 pm to 2.00 pm) although it depends on the geographical location. PV power can be low even at the noon due to bad weather condition.

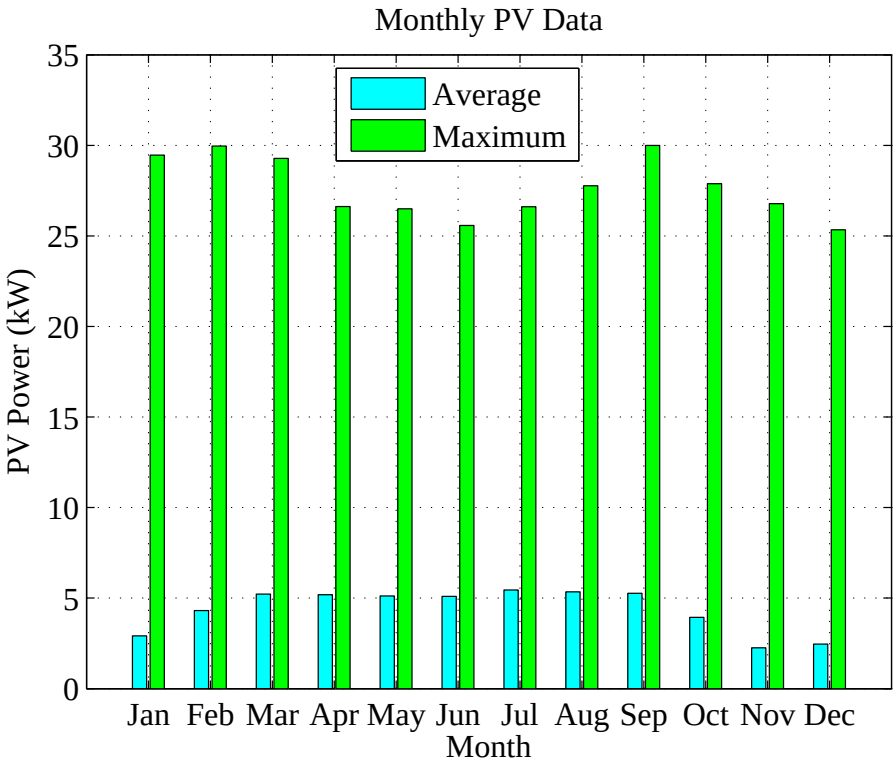

Figure 3.4. Monthly PV data throughout a year

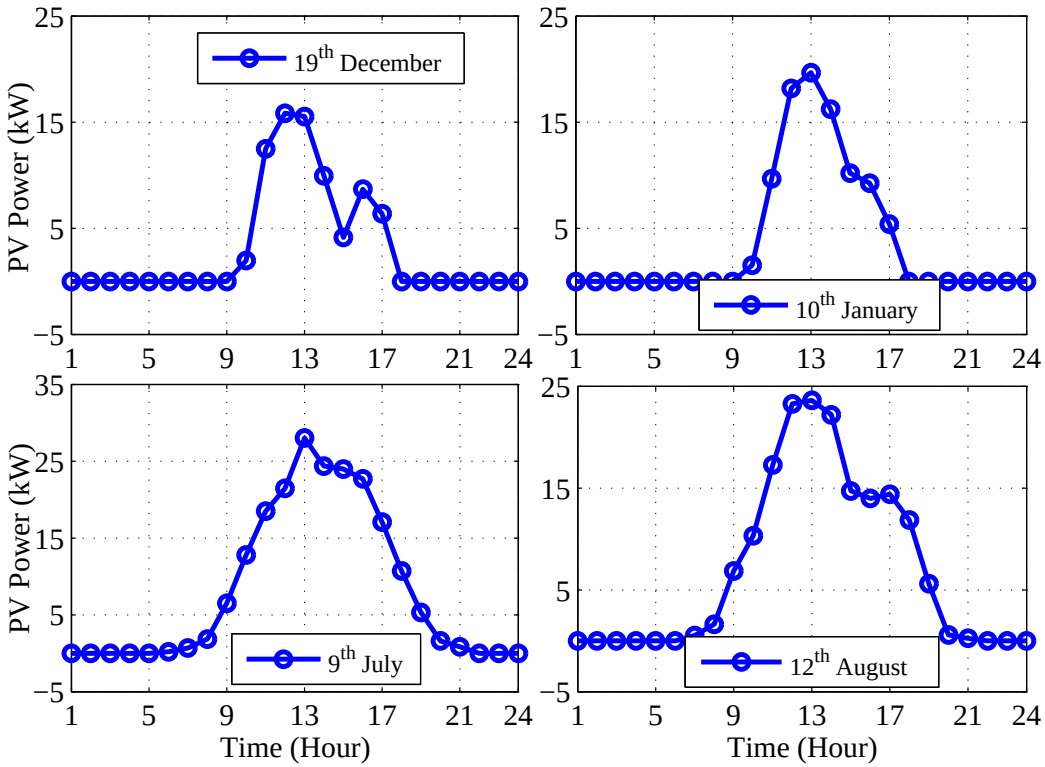

Figure 3.5. PV data in four different days

3.2.3 Diesel Generator

Generator diesel cost curve is generally represented as cubic or quadratic functions and piecewise linear functions [26], although the quadratic function more accurately models the conventional diesel generators. The cost function presents a more nonlinear nature when the actual generator behavior is considered [45]. In order to avoid wet stacking and carbon build up, the generators are supplied 30% of their rated capacity. Moreover, the generator efficiency is also higher for the operating condition near to rated load, which can be calculated by using Equation 2.2. The fuel consumption and efficiency characteristics of 30 kW and 75 kW generators are presented in Figure 3.6 and 3.7. The operating range of the 30 kW diesel generator is 9 kW to 30 kW and the operating range of the 75 kW generator is 22.5 kW to 75 kW.

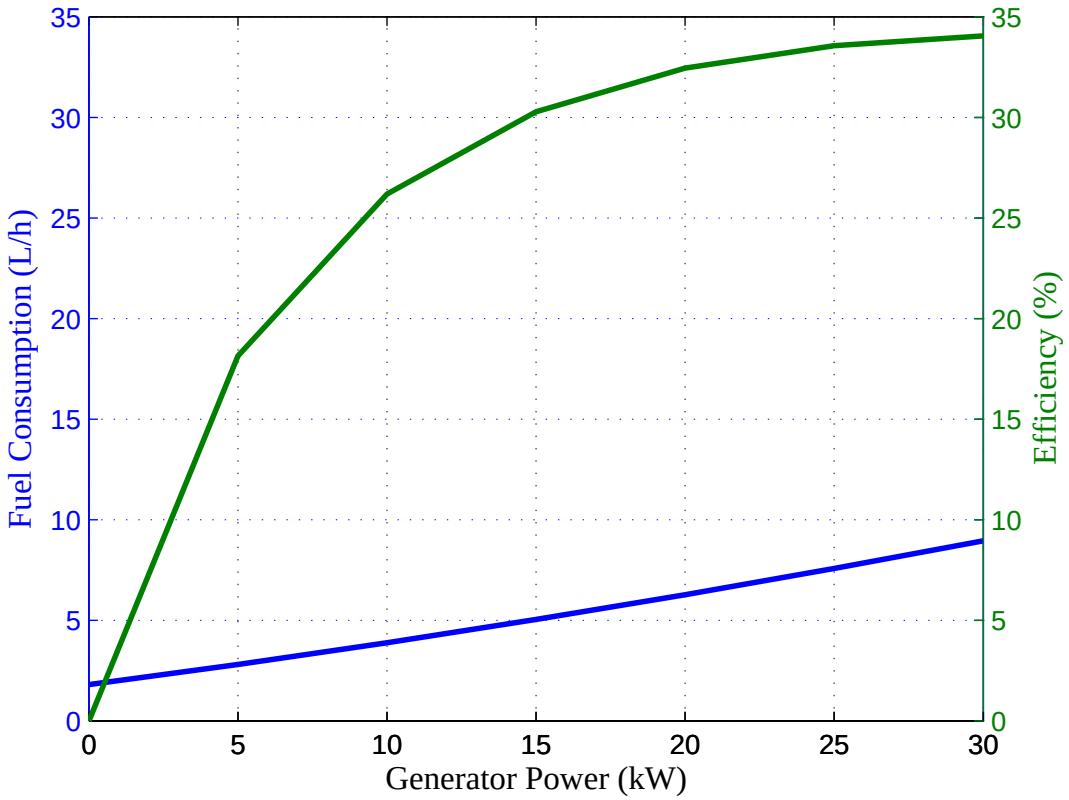

Figure 3.6. Fuel consumption and efficiency curve of 30 kW generator

In general, the total operational cost of a diesel generator depends on diesel cost, hourly replacement cost, maintenance cost, and startup and shutdown cost. The hourly replacement cost of a diesel generator depends on the lifetime working hour. 40,000 hours is the typical value between the two replacement [46][47]. The hourly replacement cost was calculated by dividing the initial investment ($) by the approximate lifetime working hours. The startup and shutdown cost is negligible in remote microgrids since the size of the generators are typically small [48]. Neglecting the maintenance cost, the total daily operational cost of the generators is given by,

$$C_g = \sum_{t=1}^{T} \sum_{k=1}^{K} [C_d(a_k P_{g,k}^2(t) + b_k P_{g,k}(t) + c_k) + C_{k,h}] U_k(t) \tag{3.1}$$

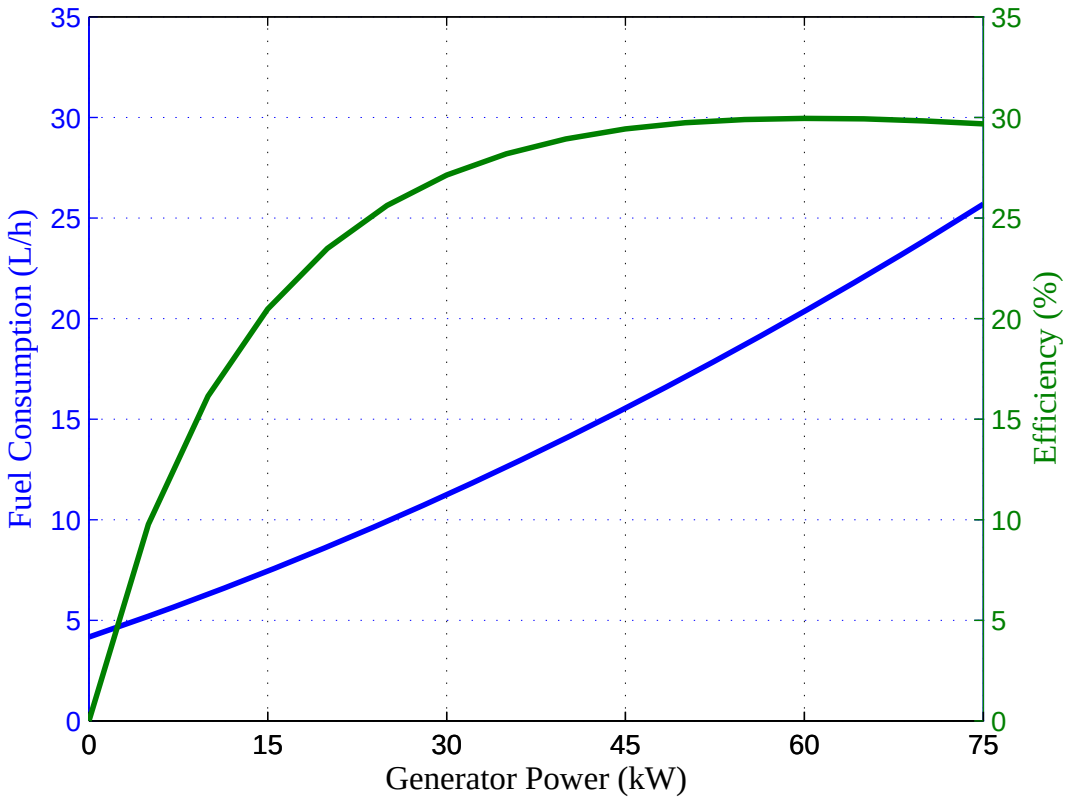

Figure 3.7. Fuel consumption and efficiency curve of 75 kW generator

where, t: Time, {1, 2, ..., T} hours; K: number of generators; $U_k(t)$: generator on/off condition at time t, (1 or 0); a_k, b_k, c_k: generator fuel curve coefficients; C_g: generator operational cost, $; $P_{g,k}(t)$: k^{th} generator power at time t, kW; C_d: diesel cost of the generators, $/gallon; $C_{k,h}$: hourly replacement cost of k^{th} generator, $/h.

3.2.4 Energy Storage System

Energy storage system (ESS) maximizes the generator fuel efficiency, minimizes fuel consumption, and utilizes the maximum available renewable energy. Moreover, it improves the system reliability and performance. However, the lifetime of energy storage systems is comparatively shorter than the other components, and the replacement cost also has a significant impact on the operational cost of the ESS and as well as the total

operational cost. The operational cost of the ESSs depends on the total life time throughput, initial investment cost, and maintenance cost. Maintenance free storage system may reduce the storage system operational cost. ESS wear cost was calculated to determine the storage system operational cost. Battery lifetime throughput is the key factor to calculate the ESS wear cost.

3.2.4.1 Wear Cost

The ESS wear cost ($\$/kWh$) can be determined by dividing the initial investment ($) by the lifetime throughput (kWh). The manufacturers provide the number of life cycles at the rated DoD, battery capacity (kWh), and initial cost information which are used to determine the ESS wear cost ($/kWh), and this is expressed by Equation (3.2) and (3.3) [49],

$$T_L = \eta_{disch} C_{ESS} N_{L,c} DoD \tag{3.2}$$

$$C_{wc,ESS} = \frac{C_i}{T_L} \tag{3.3}$$

where, C_i: ESS initial cost, $, $N_{L,c}$: number of battery life cycle, DoD: depth of discharge, %; C_{ESS}: ESS capacity, (kWh);

The rated DoD and the corresponding life cycles are different for different ESSs. Typically, the rated DoD of lead acid battery is 50%, and for lithium-ion battery, it is 90%. The rated DoD and life cycle information can be obtained from the curve provided by the manufacturer, although sometimes the manufacturer do not provide the precise

information of efficiency. In that instance, assumption was made after analyzing the similar storage system specification sheets with the efficiency information. Initial cost is another important factor to calculate ESS wear cost; higher initial cost leads to the higher wear cost and as well as the total operational cost.

3.2.4.2 ESS Operational Cost

Daily operational cost of a ESS depends on the wear cost and total throughput of the day. Considering ESS power is positive for charging and negative for discharging, the daily throughput of ESS can be determined by using Equation (3.4),

$$kWh_{TH,d} = \sum_{t=1}^{T} \frac{[|P_{ESS}(t)| - P_{ESS}(t)]\Delta t}{2} \tag{3.4}$$

where, $P_{ESS}(t)$: ESS power, kW; Δt: absolute time step of battery operation. In this study, Δt was considered 1 hour.

Daily operational cost of ESS can be obtained by using Equation (3.5),

$$C_{oc,b} = C_{wc,ESS} \cdot kWh_{TH,d} \tag{3.5}$$

3.3 Evaluation of Different Energy Storage Technology

In the beginning of this thesis, the specification sheet from different energy storage manufacturers were analyzed to calculate the wear cost. The data of battery charging and discharging power were also accumulated to simulate the optimization model. The evaluation of the storage systems was done for remote microgrids EMS considering the generators fuel consumption, storage device lifetime, and the total system operational cost.

3.3.1 Mathematical Model of the EMS

To ensure optimal operation of a remote microgrid, the EMS performs optimization and schedules the distributed energy resources accordingly. In this study, a deterministic optimization model was used to optimize the system, developed by Santosh et.al. [22].

3.3.1.1 Objective Function

The objective function of this optimization problem is the weighted sum of the generators operational cost (C_g) and the batteries operational ($C_{oc,b}$) cost. In the benchmark, all the other costs were considered constant including the maintenance cost. So, the objective function was formed by using Equation (3.1) and (3.5) which is to,

$$Minimize, W_1 \times C_g + W_2 \times C_{oc,b} \tag{3.6}$$

where, $W_1 + W_2 = 1$. The weight W_1 represents the weight of generator operational cost and W_2 represents the weight of the battery operational cost. W_1 and W_2 determine the generators fuel consumption and battery throughput accordingly. For example, when W_1 is 1 and W_2 is 0, less fuel will be consumed (generator operation cost will be the lowest, as it is carrying more weight) and more battery throughput will be used that leads to shorter battery lifetime.

3.3.1.2 Equality Constraint

In each hour of a day, the total amount of power from the generators, battery and PV system was equal to the load power which is given by,

$$\sum_{k=1}^{K} P_{g,k}(t) + P_{b/UC}(t) + P_{PV}(t) = P_D(t), t \in T \tag{3.7}$$

where, t: Time, {1, 2, ..., T} hours; K: number of generators; $P_{g,k}(t)$: k^{th} generator power at time t, kW; $P_{b/UC}(t)$: battery/UC power at time t, kW; $P_{PV}(t)$: photovoltaic power at time t, kW ; $P_D(t)$ is the load demand at time t, kW.

3.3.1.3 Inequality Constraints

The diesel generator were operated at certain load to maintain high fuel efficiency.

$$P_{g,k,min} \leq P_{g,k}(t)U_k(t) \leq P_{g,k,max}, \forall t \in T \tag{3.8}$$

where, $U_k(t)$: Generator on/ off condition at time t, (1 or 0); $P_{g,k,min}$: minimum power from k^{th} generator; $P_{g,k,max}$: maximum power from k^{th} generator.

The storage device lifetime depends on the allowable SoC $(= 1 - DoD)$. If a battery is operated below its allowable SoC range then its lifetime decreases significantly. For different types of energy storage technology, allowable SoC range was different.

$$SoC_{min} \leq SoC(t) \leq SoC_{max}, \forall t \in T \tag{3.9}$$

where, $SoC(t)$: battery/UC SoC at time t; SoC_{min}: minimum SoC of battery/UC; SoC_{max}: maximum SoC of battery/UC;

Charging (ch) and discharging (disch) power of a battery/UC was in a specific range to prolong the lifetime by preventing over charging and discharging.

$$P_{b/UC,disch} \leq P_{b/UC}(t) \leq P_{b/UC,ch}, \forall t \in T \tag{3.10}$$

where, $P_{b/UC,disch}$: battery/UC discharging power, kW; $P_{b/UC,ch}$: battery/UC charging power, kW.

The optimization problem was solved by using the IBM ILOG CPLEX software to minimize the objective function with above constraints.

3.4 Incorporation of the Schiffer Model in the EMS

The Schiffer model consists of SoC weight factor (W_{SoC}) and acid weight factor (W_{Acid}). For the sake of simplicity, only W_{SoC} was considered in the EMS. W_{SoC} has a significant impact in the microgrids EMS. In [22], W_{SoC} was considered for remote microgrid day ahead EMS without considering it in the objective function. In that approach, it may not reflect the accurate effects on the EMS, and may deviates the scheduling results of the distributed energy resources. According to [18], W_{SoC} should be calculated after each cycle of operation to obtain the weighted throughput. In a day ahead EMS, it is very complicated to calculate W_{SoC} on hour basis and incorporate in the EMS. For simplicity, a modified W_{SoC} was incorporated in the EMS so that the effects of this factor can be analyzed more accurately.

3.4.1 Modified SoC Weight Factor, $W_{SoC,m}$

The SoC weight factor (W_{SoC}) is significantly influenced by Δt_{SoC}. The value of W_{SoC} increases linearly over the period of battery operation and reset to the initial value after one full charge [19][18]. The value of W_{SoC} over a small period of time is nearly same. For the simplicity, an average value of W_{SoC} was considered in the objective

function. In the modified form, the next day W_{SoC} was calculated from the average W_{SoC} of the present day as equation (3.11),

$$W_{SoC,m}(d+1) = \sum_{t=1}^{T} \frac{W_{SoC}(t,d)}{T} \tag{3.11}$$

where, t: time, hour and d: number of day.

3.4.2 Weighted Battery Throughput

Battery weighted throughput was obtained from the SoC weight factor $W_{SoC,m}$ and the actual throughput which can be determined by using Equation 3.4 and 3.11

$$W_{kWh}(d) = W_{SoC,m}(d) \cdot \sum_{t=1}^{T} \frac{[|P_b(t)| - P_b(t)]\Delta t}{2} \tag{3.12}$$

where, $W_{kWh}(d)$: daily weighted battery throughput, kWh; $P_b(t)$: battery power, kW. The weighted throughput is always higher than the actual value since $W_{SoC,m}$ is greater than unity. A battery is considered to be expired when the amount of weighted throughput have reached to the calculated lifetime throughput. Higher value of $W_{SoC,m}$ leads towards the high weighted throughput, consequently reduces the battery lifetime. $W_{SoC,m}$ not only degrades the battery faster but also increases the operational cost. The battery operational cost can be determined from the battery wear cost and weighted battery throughput by using the following equation.

$$C_{oc,b,m}(d) = C_{wc,bat} \cdot W_{kWh}(d) \tag{3.13}$$

where, $C_{wc,bat}$: battery wear cost which was considered as the PbA battery in the

Task 1.

3.4.3 Modified Objective Function

The modified objective function was obtained by considering $W_{SoC,m}$ in the Equation 3.6 which can be given by

$$Minimize, W_1 \times C_g + W_2 \times C_{oc,b} \times W_{SoC,m} \tag{3.14}$$

Previously, the priority of the objectives was determined by the weight W_1 and W_2 but in this work, $W_{SoC,m}$ was included in the modified objective function to adjust the priority when battery degradation is higher. Besides the higher value of W_2, $W_{SoC,m}$ put more weight to the battery operational cost, that increases the generator operational cost as well as the fuel consumption. Comparatively higher value of W_2 and lower value of $W_{SoC,m}$ can provide better solution in terms of the system operational cost and battery lifetime, although the fuel consumption may increase slightly. However, the low diesel price can be effective but it depends on the providers. The more effective solution is to reduce the value of $W_{SoC,m}$. To do so, different strategies were analyzed in the Section 3.5. In such ways, battery life time can also be improved.

3.5 Case Study

From the Section 2.4.1.1, it can be observed that the value of W_{SoC} can be reduced either by operating the battery at higher SoC range or by minimizing Δt_{SoC} i.e frequent full charging. Hence, there is an associated cost to charge the battery by the diesel generators as well as the fuel consumption. To obtain a cost effective battery cycling strategy, different approaches were analyzed in this thesis which are described in this

section as case study. There are two case studies which were considered and each case have five different sub cases.

3.5.1 Case I: Objective Function without W_{SoC}

In case I, W_{SoC} was excluded in the the objective function, but at the end of the calculation it was considered in the EMS. There were different battery cycling strategies to minimize the value of W_{SoC} which were considered in the five subcases. Different periodical cycling strategies were considered in the subcases.

- **Case I (a)**: No Charging Cycle

  In Case I (a), simulations were done without considering any cycling strategy.

- **Case I (b)**: Weekly Charging

  This case is the combination of Case I (a) and weekly cyclic charging strategy. Battery underwent one full charge at the first hour of a week. The required battery power depends on the final hour SoC of the 7^{th} day.

- **Case I (c)**: Bi-weekly Charging

  In Case I (c), it was considered that the battery was fully charged after every 2 weeks.

- **Case I (d)**: Monthly Charging

  After each month of operation, the battery was considered to be full charged in Case I (d).

- **Case I (e)**: Threshold Crossing

In Case I (e), threshold value of W_{SoC} was considered to schedule the battery for full charging. In this strategy, the battery went through a charging procedure when the value of W_{SoC} was equal to or greater than the threshold value. Different threshold values were considered to find the optimum value with the minimum operational cost and the generators fuel consumption.

3.5.2 Case II: Objective Function with W_{SoC}

In Case II, W_{SoC} was incorporated in the objective function and simulations were done thereafter. Similar to Case I, five sub cases were also analyzed in Case II.

3.5.3 Battery Charging Procedure

In periodically cycling strategy, the battery was fully charged up after the predefined period (ex. one week). The amount of power to full charge (SoC=1) the battery ($\Delta P(t)$) after that period was calculated by using Equation (3.15)

$$SoC(t+1) = SoC(t) + \frac{\eta \Delta P(t) \Delta t}{C_b} \tag{3.15}$$

where, $SoC(t)$: SoC at hour t (for weekly charging, it is the final hour SoC of 7^{th} day; $SoC(t+1)$: next hour SoC (first hour SoC at 8^{th} day for weekly charging); $P_b(t)$: battery charging power (kW); C_b: battery capacity, (kWh); Δt: charging duration; η: charging efficiency;

Afterwards, the calculated power (ΔP) was equally added up with the first two hours load (P_L) of 8^{th}, 16^{th} and 31^{st} day for weekly, biweekly and monthly cycling operation respectively. In the case studies, it was considered that the charging of the batteries was done by the generator(s).

$$P_{L,1} = P_{L,1} + \frac{\Delta P}{2}; P_{L,2} = P_{L,2} + \frac{\Delta P}{2}$$

where, $P_{L,1}$ and $P_{L,2}$ are the load at hour 1 and 2 respectively at next day after one periodic cycle.

In case auto charging (threshold crossing), the charging strategy is same as the periodically charging strategy.

CHAPTER 4 RESULT AND ANALYSIS

This chapter describes the results obtained from the simulation of the optimization problem by using IBM ILOG CPLEX 12.6.1 software. Section 4.1 represents the wear cost of the storage devices with associated information. Section 4.2 evaluates the effectiveness of different batteries. Followed by, the use of modified optimization model, considering how including the Schiffer Ah model in the objective function impacts the operation of remote microgrids.

4.1 Storage Device Wear Cost

In this section, the wear cost of PbA, $LiFePO_4$, Li-ion, Hybrid ion batteries, and ultracapacitor (UC) are presented. The battery/UC bank was designed considering the peak load demand, 64 kW. Wear costs were calculated by using the Equation 3.3.

Table 4.1. Storage device information [10], [50]–[56]

Type	$\eta_{dis}, \%$	Rated DoD, %	Life cycles	Initial cost, $	Lifetime throughput, kWh	Wear cost, $/kWh
PbA	90	50	1,000	32,430	64,087	0.506
$LiFePO_4$	90	90	3,000	91,650	192,065	0.477
Li-ion	92.5	90	5,000	36,000	319,680	0.112
Hybrid ion	90	80	4,000	46,605	260,403	0.178
UC	95	90	1 million	1,835,600	63,984,780	0.028

The required storage size (kWh) depends on rated DoD and discharging efficiency. The manufacturer didn't provide the precise information about the discharging efficiency of $LiFePO_4$, hybrid ion batteries, and UC; on that circumstance, the discharging efficiency were considered 90%, 90% and 95%, respectively.The storage device wear cost was calculated from the available data of DoD, life cycles, efficiency, and initial cost. All the associated costs were considered in the U.S. dollar ($).

4.2 Feasibility Analysis of the Storage Devices

This section analyze the feasibility of five different types of energy storage devices that used in remote microgrids energy management system (EMS). Section 4.2.1 describes the comparison of the fuel consumptions while considering different storage devices in the EMS. Comparison of lifetime of the storage devices and the system operational cost are presented in the Section 4.2.2 and 4.2.3 respectively.

4.2.1 Fuel Consumption and Battery/UC Throughput

The yearly fuel consumption of the diesel generators depends on the amount of battery throughput that utilized by the EMS and it varies for the different values of weight W_1 which are presented in the Figure 4.1 and 4.2. When the fuel consumption of the diesel generators increases, the battery/UC throughput decreases and vice-versa. Wear cost is an important factor to access more throughput from a battery/UC. Due to the lowest wear cost ($0.028/kWh), the EMS utilized more throughput from the UC than the other storage devices for each value of W_1, and consequently, fuel consumption of the generators was the lowest. Compared to other storage devices, generators consumed at least 3.15% less fuel when the UC was used. Among all the batteries, fuel consumption was the lowest and the yearly throughput was the highest while Li-ion battery was used in the EMS and this was because of the lower wear cost. The yearly battery throughput of the PbA and $LiFePO_4$ batteries and consequence fuel consumption were remain almost the same for the different values of W_1 because of the narrow margin of their wear cost.

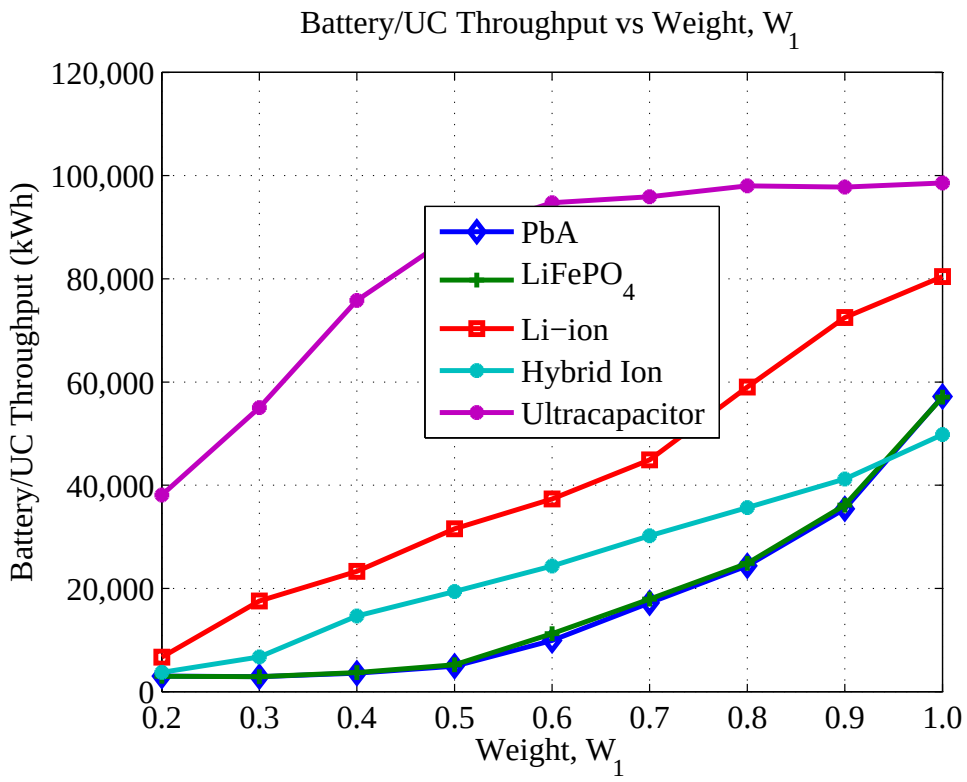

Figure 4.1. Yearly battery/UC throughput

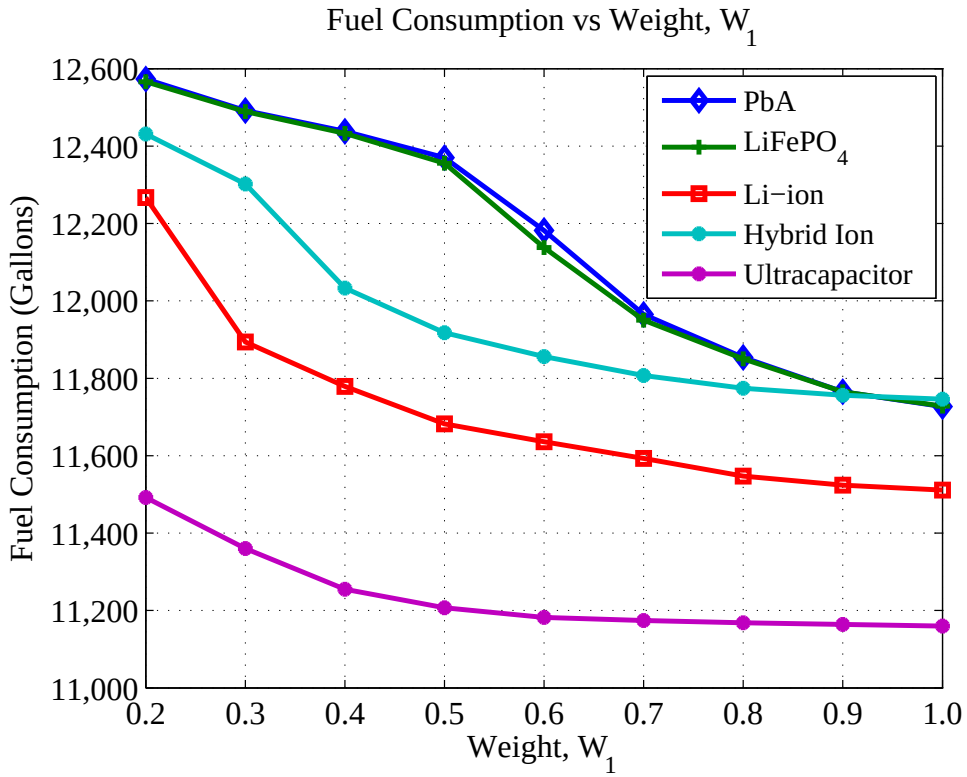

Figure 4.2. Yearly fuel consumption of the generators

4.2.2 Battery/UC Lifetime

The lifetime of a battery/UC was determined by comparing the yearly throughput with the estimated yearly throughput. The estimated throughput was obtained from the data in manufacturer sheets. However, the lifetime of a battery/UC depends on the total throughput utilizes by the EMS. Excess amount of throughput leads to a shorter lifetime. The value of weight, W_1 influences the battery/UC lifetime. Higher the value of W_1, higher the battery throughput, and lower the battery lifetime. Figure 4.3 shows the lifetime curves of different energy storage devices. The lifetime was considered equal to its float life if the EMS could not utilize the total estimated lifetime throughput over this period.

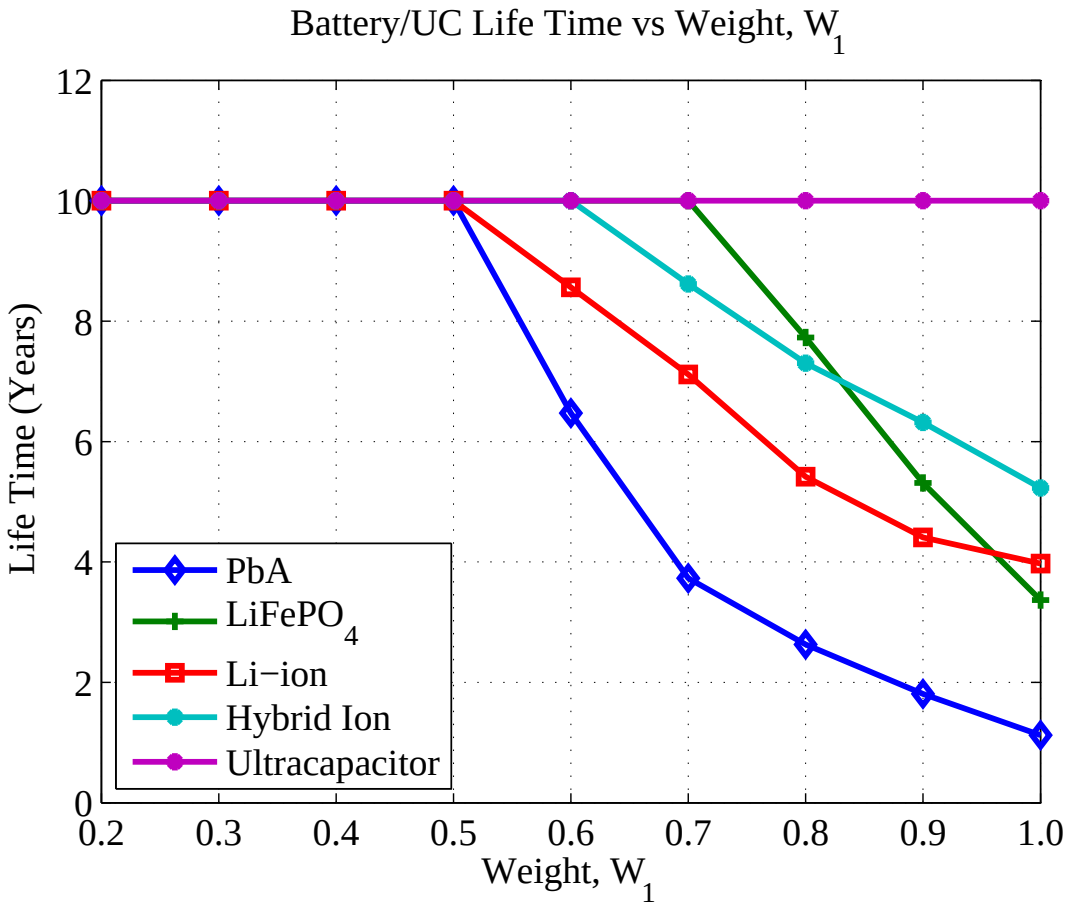

Figure 4.3. Storage devices lifetime

In case of UC, due to high amount of unutilized energy, the estimated lifetime was 10 years for different values of W_1. PbA battery had the shorter lifetime than the other batteries and hybrid ion batteries had higher lifetime than the PbA and Li-ion for $W_1 > 0.5$.

4.2.3 Operational Cost

The total cost of operation consists of the individual operating cost of generators, battery/UC, and the float life cost of the battery/UC. The float life cost is the value of the energy that being unused the battery/UC expires . Typically, the float life of a PbA battery is 10 years [57]. For example, estimated yearly throughput of PbA is 6,408.7 kWh. At W_1 = 0.3, the EMS utilized 2,909 kWh i.e. 3,046.7 kWh is being unused of cost $1,771 (wear cost: $0.506/kWh).

Figure 4.4 shows that, the total operational cost was decreased with the increment of weight W_1 while using the UC. The optimal range of weight W_1 was found in between 0.5 to 0.8 for most of the batteries. Total cost of operation was almost 3 times higher for UC at each value of W_1, although the value of the UC wear cost ($0.028/kWh) is the lowest among the energy storage devices. This was because of high float life cost. Due to the high float life cost of UC, the total operational cost of the microgrid system was too high. High initial cost of UC ($1,835,600 for 64 kWh) was the key factor for the high yearly operational cost. The estimated yearly throughput of UC is 6,398,478 kWh (10 years float life [10]) but the EMS utilized maximum 98,575 kWh, which leads to the high float life cost and the total operational cost as well. Therefore, UC storage system is not a viable option in this case.

At different values of W_1, the total operational cost was comparatively higher for

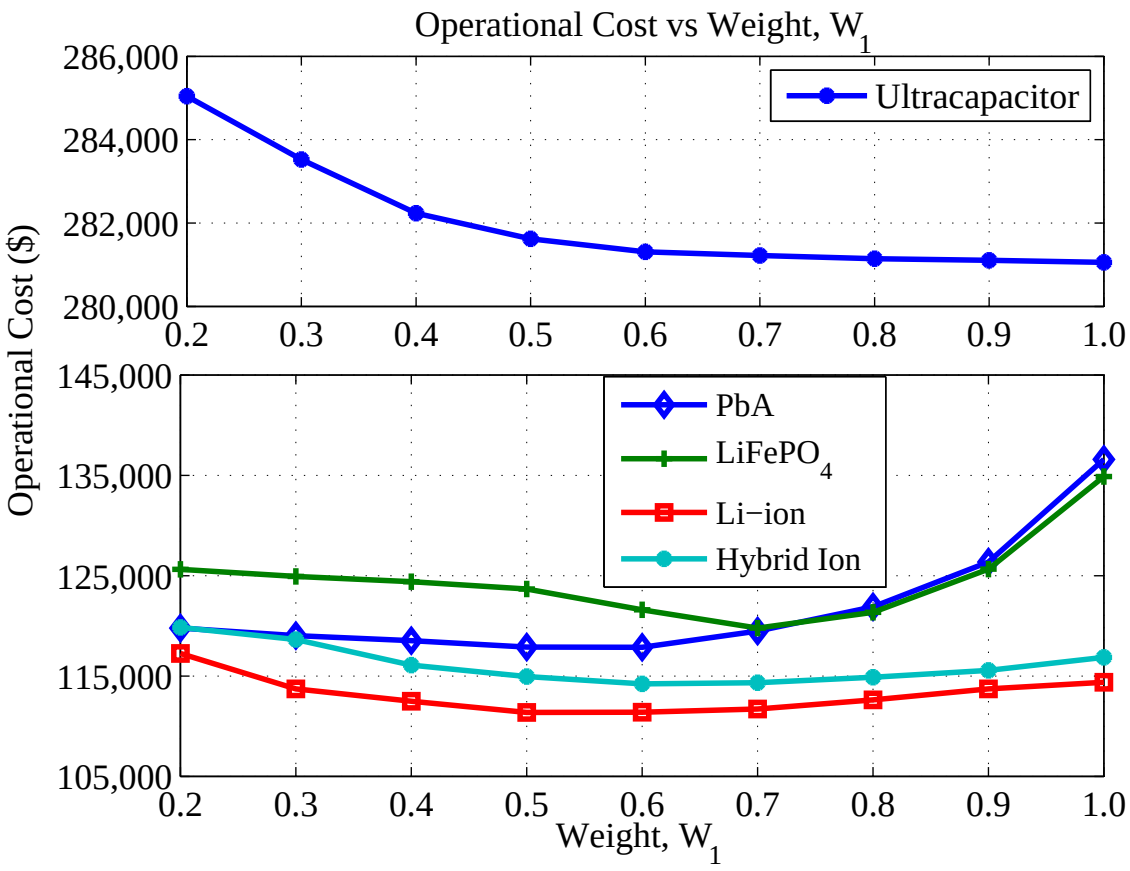

Figure 4.4. Yearly operational cost

using the PbA and $LiFePO_4$ than the other two types of battery due to the high wear cost (Figure 4.4). According to the results, the Li-ion and hybrid ion batteries were more potential storage devices for remote microgrids EMS. In both instances, estimated lifetime was 10 years with a negligible float life cost. However, the Li-ion battery was found to be 2.55% ($2,812) more cost effective than the hybrid ion battery. Additionally, the yearly fuel consumption was found to be about 1.5% (171 gallons) lower in the system while the Li-ion battery was used. In this study, all the analysis are based on the theoretical data. In real life operation, the performance of a particular battery may differ.

Table 4.2. Yearly simulation for Case I (a)

W_1	Yearly fuel consumption, $gallons$	Yearly throughput, kWh	Float life cost, $	Total operational cost,$	Weighted yearly throughput, kWh	Weighted Float life cost,$	Weighted Total operational cost, $
0.1	14,144	3,058	1,696	133,945	3,276	1,585	13,3945
0.2	14,120	2,962	1,744	133,723	4,579	926	133,723
0.3	14,067	2,961	1,745	133,222	12,046	0	136,074
0.4	14,027	3,858	1,291	132,398	27,3690	0	143,447
0.5	13,978	5,000	713	132,398	32,448	0	145,574
0.6	13,811	9,014	0	132,147	62,369	0	159,158

4.3 Incorporation of W_{SoC} in the EMS

In this section, different subcases were analyzed considering total operational cost and generators fuel consumption. The battery weighted throughput and lifetime for different subcases are included in the appendix. The operational cost and fuel consumption were calculated in yearly basis.

4.3.1 Case I: Objective Function without $W_{SoC,m}$

In case I, battery underwent a full charge periodically so that the value of state of charge (SoC) weight factor, $W_{SoC,m}$ can be reduced.

Table 4.2 presents the simulation results in Case I (a). The minimum operational cost was found at W_1=0.6 when $W_{SoC,m}$ was not considered in the EMS. However, the optimum point was shifted to W_1=0.2 due to the consideration of $W_{SoC,m}$ in the EMS. It was the consequence of the high value of W_{SoC} at W_1 >0.3. W_{SoC} increased till the end of the year and never fall back to the initial value (=1) when W_1 was 0.5 and 0.6. This was due to the lack of full charge throughout the year. Figure 4.5 shows the $W_{SoC,m}$ and corresponding SoC profile in Case I (a) at three different values of W_1. It is clear to see that for W_1= 0.5 & 0.6, the battery SoC did not reach the full charge region (i.e., SoC=1.0)

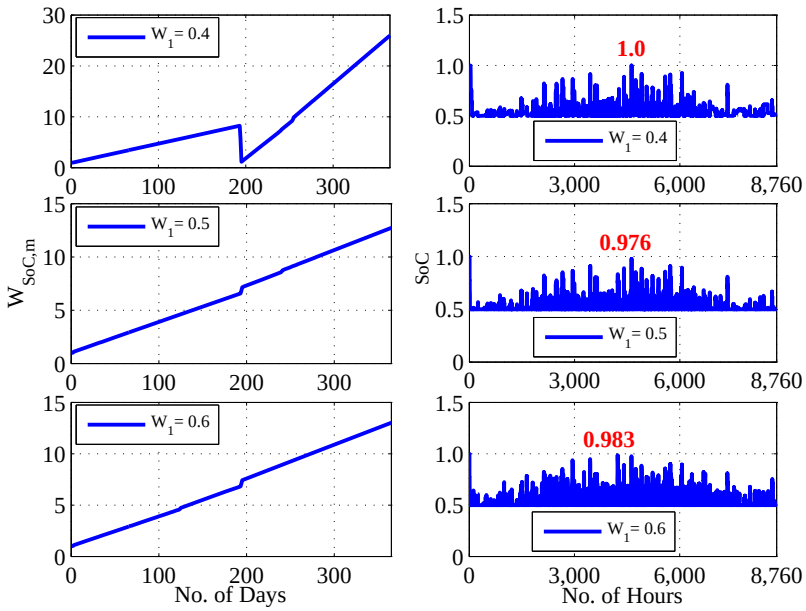

Figure 4.5. $W_{SoC,m}$ and SoC plots for different weight, W_1 in Case I (a)

after first few cycle. As a result, Δt_{SoC} gradually increased until the end of the year. The battery SoC reach 1.0 once in Case I (a) with W_1=0.4 which also reflect in the values $W_{SoC,m}$ at that point.

In Case I (a), the optimum total operational cost was found about $600 higher than the Case I (b), (c), and (d). Among these cases, the lowest operational cost ($133,155) was obtained in Case I (b). Figure 4.6 shows the yearly total operational cost curves for all the cases and weight, W_1. The optimum operating point for case I (b), (c), and (d) was at W_1=0.3 but in case I (a), it was at 0.2. Fuel consumption of the generators was found almost the same at different cases and different values of weight, W_1. Figure 4.7 shows the generator fuel consumption.

In Case I (e), the minimum operational cost was found at $Th, W_{SoC,m}$=1.05 which was $133,034 (Figure 4.8). In the same point, the fuel consumption by the generators was also the lowest 14,052 gallons (Figure 4.9).

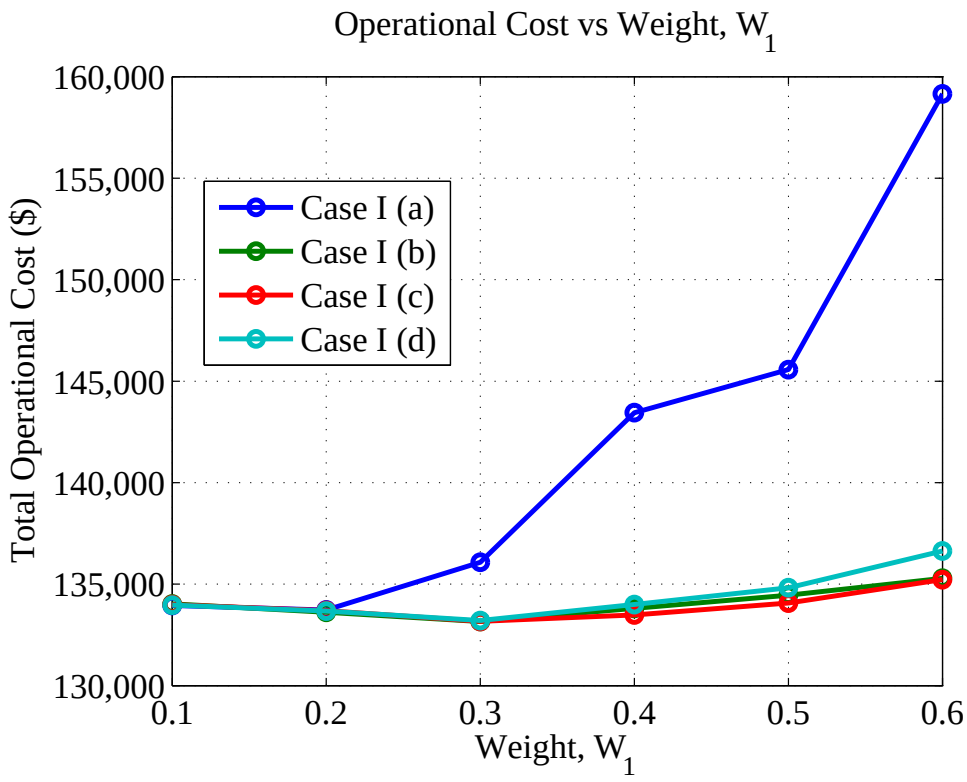

Figure 4.6. Yearly total operational cost in Case I (a)-(d)

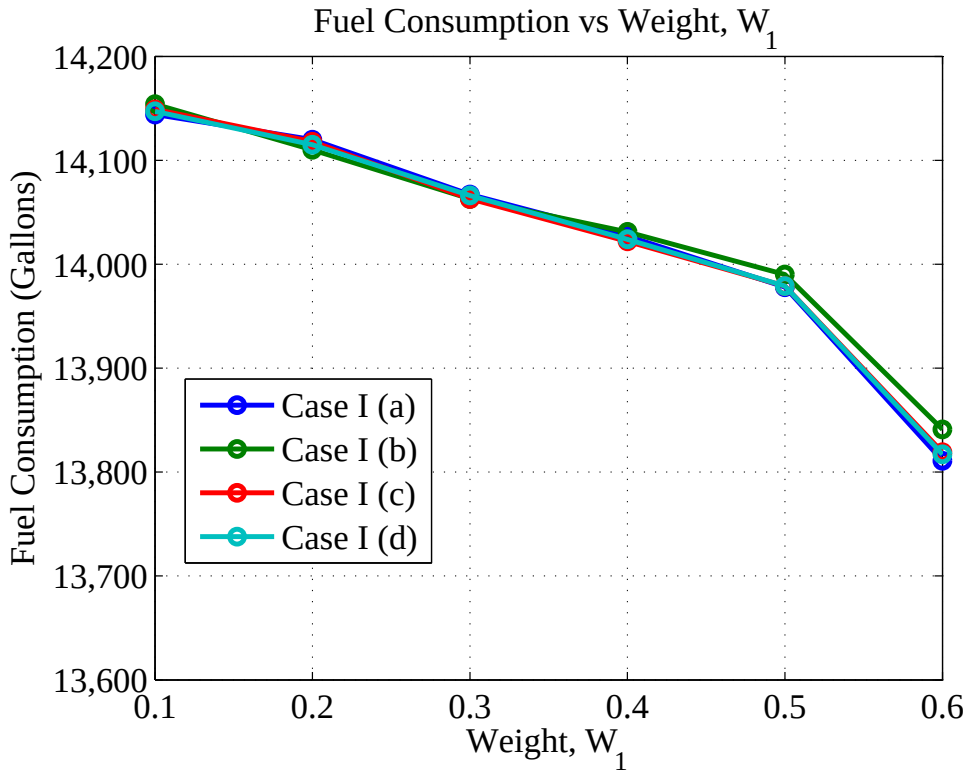

Figure 4.7. Yearly generators fuel consumption in Case I (a)-(d)

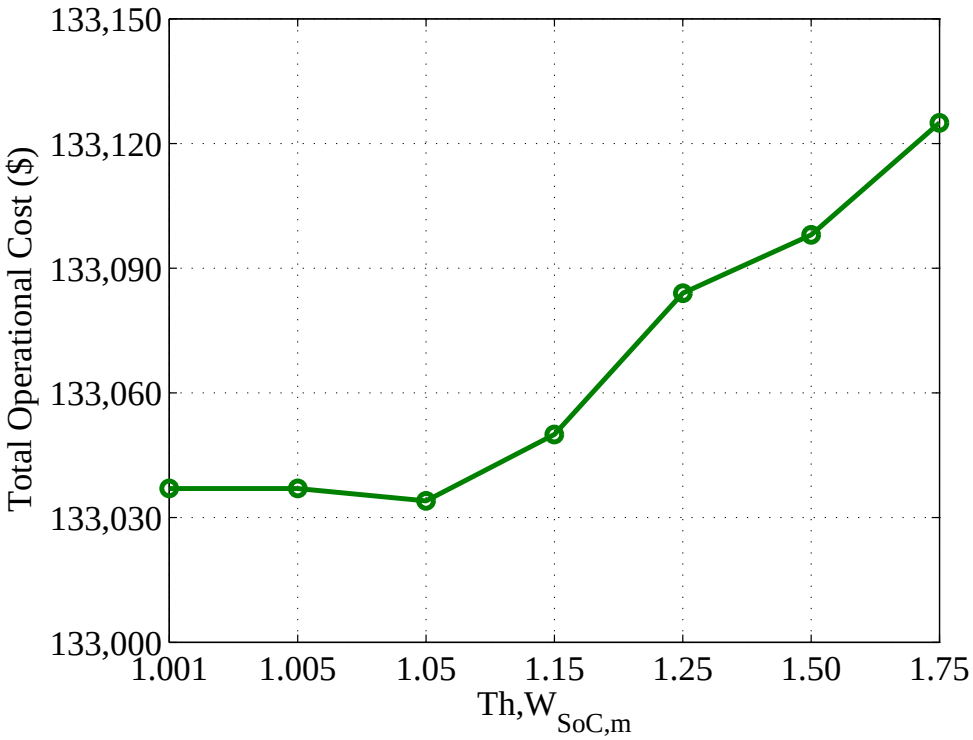

Figure 4.8. Yearly total operational cost in Case I (e)

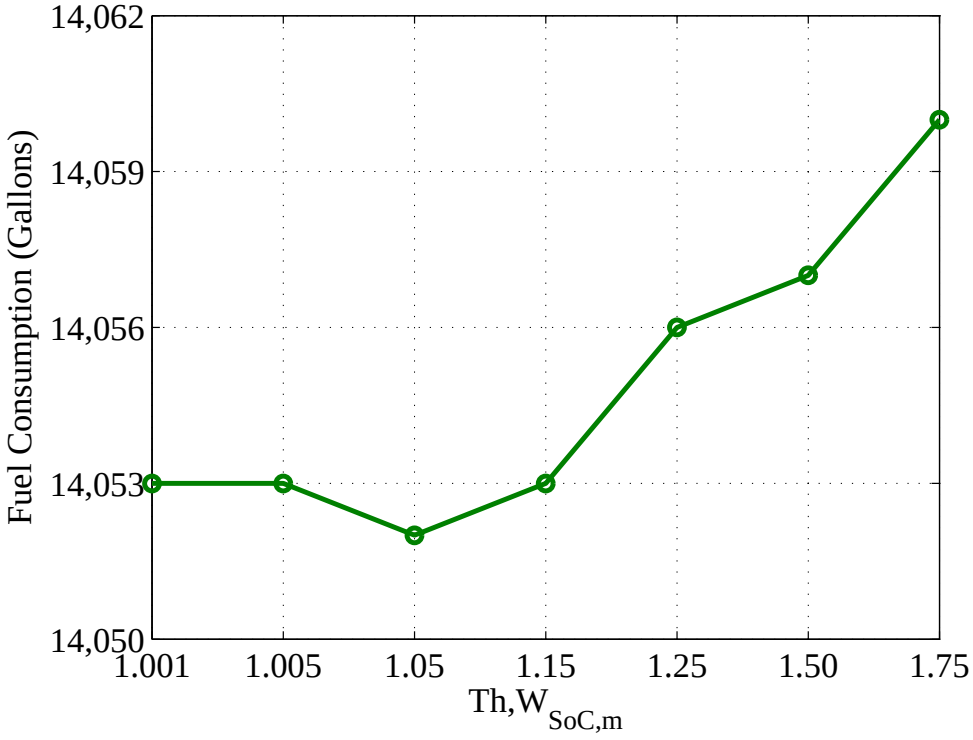

Figure 4.9. Yearly generators fuel consumption in Case I (e)

4.3.2 Case II: Objective Function with $W_{SoC,m}$

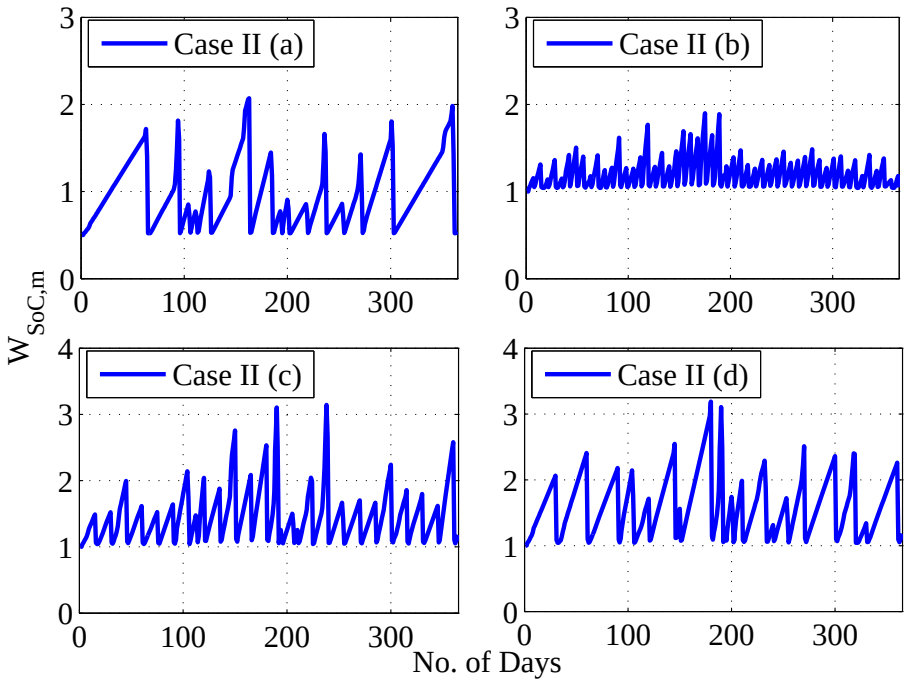

Figure 4.10. $W_{SoC,m}$ plots at W_1=0.4 in Case II (a)-(d)

From Case II (a) to (d), the minimum operational case was found at W_1=0.4 and considered it as the optimum operational point. The value of $W_{SoC,m}$ was the highest in Case II (a) due to lack of regular full charging of the batteries. It was obvious that $W_{SoC,m}$ would be lower in Case II (b) which was weekly cycling strategy and then in the bi-weekly and monthly cycling strategy. Figure 4.10 illustrates the $W_{SoC,m}$ in Case II (a), (b), (c), and (d). The average value $W_{SoC,m}$ in Case II (c) and (d) were about 1.4 and 1.6 respectively. $W_{SoC,m}$ remains high over longer period of time in Case II (d).

However, the total operational cost depends on the value of $W_{SoC,m}$; higher value leads towards the higher cost. Compared to Case II (a), the total operational cost in the other cases were lower although the difference was small (Figure 4.11). In Case II (b) and (c), the total operational cost was almost the same ($3 higher in Case II (a)). By using

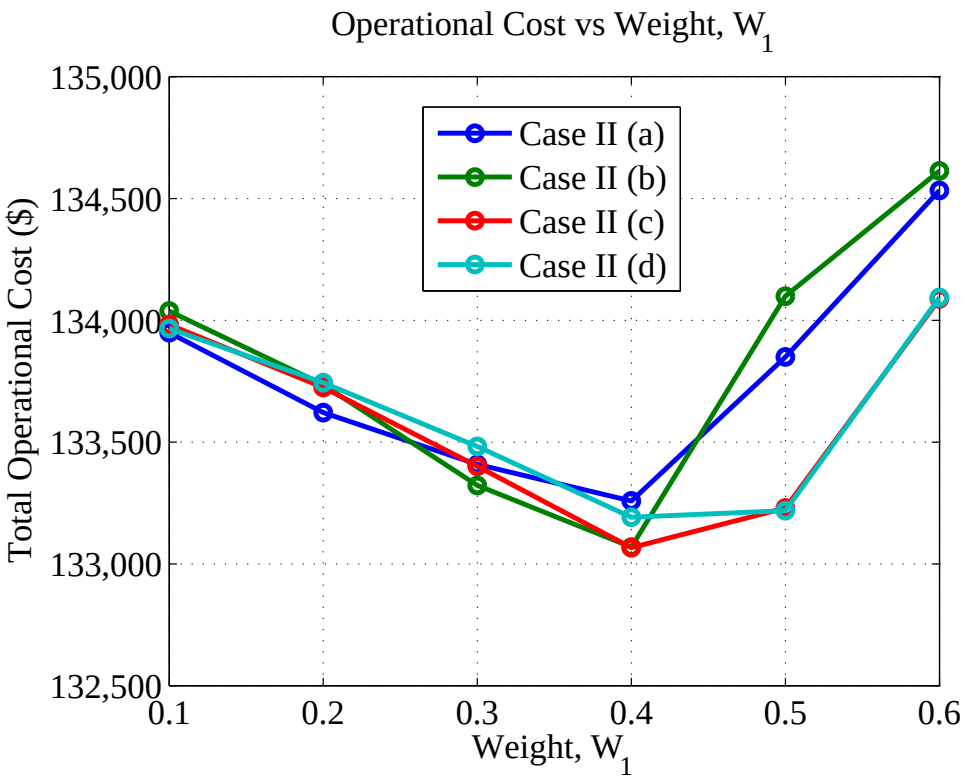

Figure 4.11. Yearly total operational cost in Case II (a)-(d)

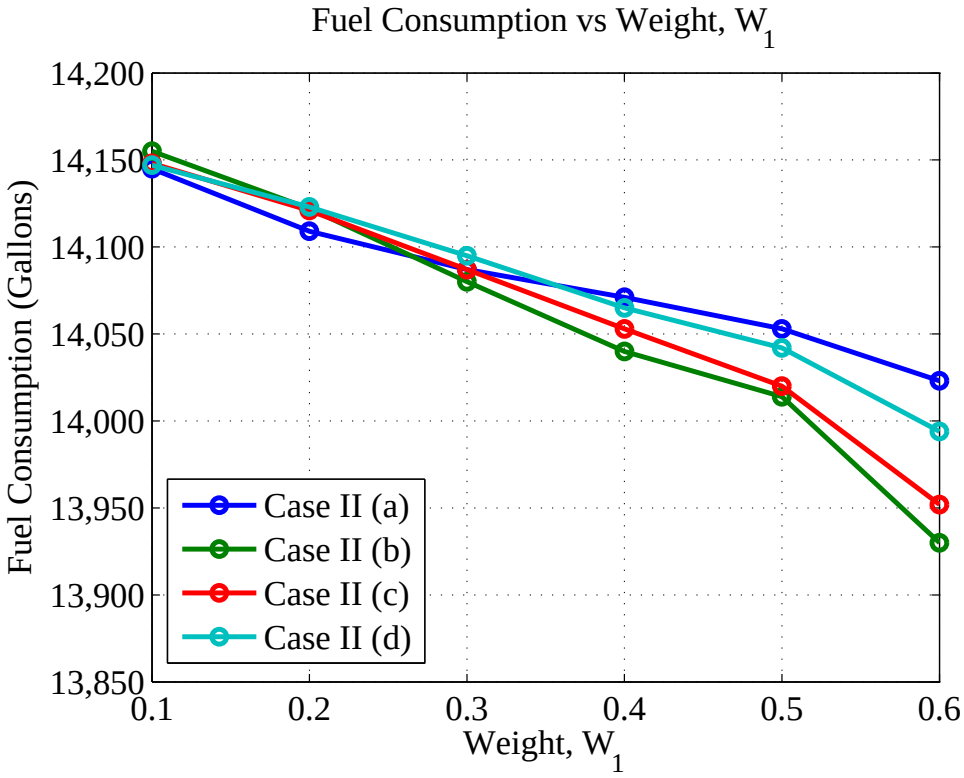

Figure 4.12. Yearly generators fuel consumption in Case II (a)-(d)

bi-weekly charging approach (Case II (b)), the yearly total operational cost can be reduced by $192 at the optimum operating point, W_1=0.4. In the same point, the fuel consumption was the lowest in Case II (b). Therefore, in Case II (b), operational cost was $3 higher than Case II (c), but the generator fuel consumption was lower by 13 gallons. Compared to Case II (a), the fuel consumption in the system can be reduced by 22 gallons in Case II (c) (Figure 4.12).

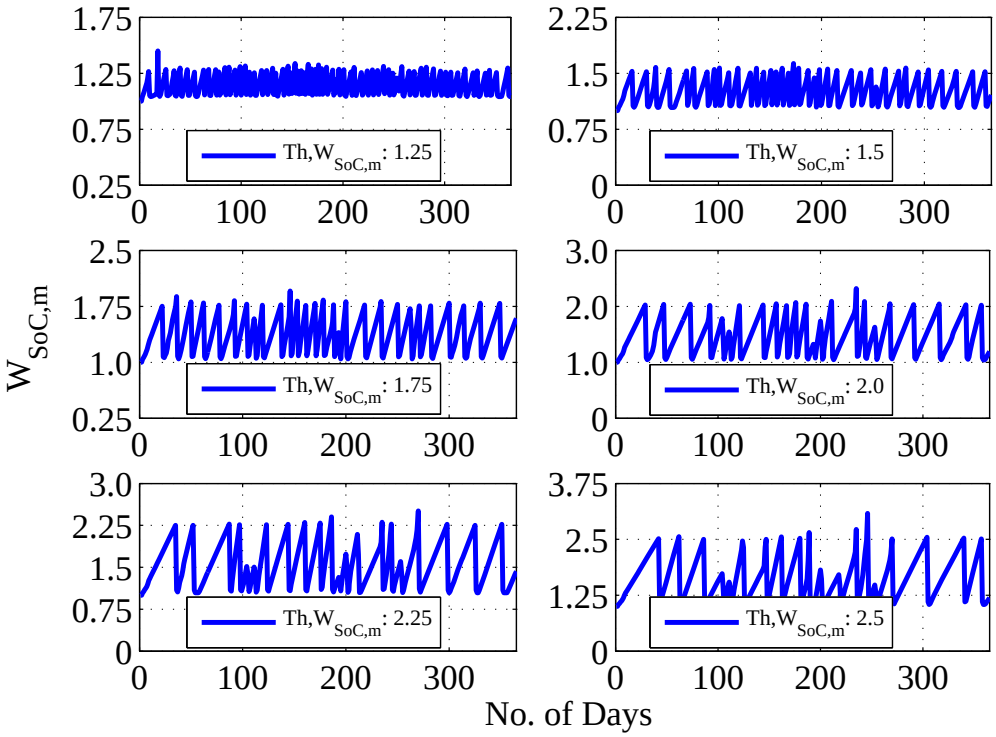

Figure 4.13. $W_{SoC,m}$ plots for the different values of $Th, W_{SoC,m}$ at $W_1 = 0.4$ in Case II (e)

Auto cycling was considered in Case II (e) which is such that the battery undergoes the charging process to reach the full charge state (SoC=1) when $W_{SoC,m}$ is equal or higher than a threshold value ($Th, W_{SoC,m}$). The charging procedure of the battery is similar as the case II. The value of $Th, W_{SoC,m}$ was considered from 1.25 to 2.5 with 0.25 interval to find an optimum value.

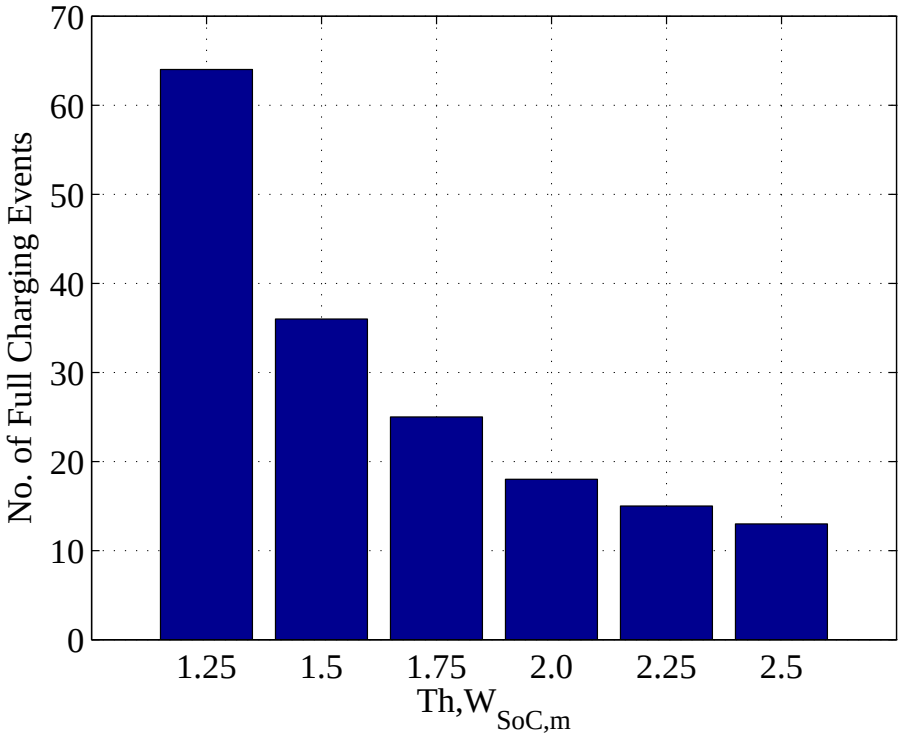

Figure 4.14. No. of cycling charges in Case II (e)

In Case II (a)-(d), the optimum operating point (minimum operational cost) was found at weight, W_1=0.4 and the value of W_1 remained the same for Case II (e). The value of $W_{SoC,m}$ is an important factor to obtain the lower operational cost. Figure (4.13) $W_{SoC,m}$ variation within the threshold value; however, in some cases, there were small sharp peaks in $W_{SoC,m}$ beyond the threshold value due to the number of bad charging (incomplete full charging) during that days.

However, the number of charging cycles increases with the decrement of $Th, W_{SoC,m}$. Diesel generators fuel consumption also increases and impacts the total operational cost. Figure 4.14 shows the number charging cycles required for different values of threshold values. The highest number of charging cycle were 66 at $Th, W_{SoC,m} = 1.25$ and the lowest were 12 at $Th, W_{SoC,m} = 2.5$.

The fuel consumption depends on the battery throughput since the total load was supplied by the generators and/or battery. Except at $Th, W_{SoC,m} = 1.25$, generators fuel consumption was higher for the higher value of $Th, W_{SoC,m}$ and this is because of high number of cycling charging. Whenever $Th, W_{SoC,m}$ increases, the utilization of the battery throughput decreases; however, it increases the fuel consumption slightly but the amount is not that significant. In Case II (a), generators fuel consumption was 14,071 gallon in the optimum point at weight, $W_1 = 0.4$. At the same point in Case II (e), the fuel consumption was lower than Case II (a) for all the values of $Th, W_{SoC,m}$ but at the value of 1.5, fuel consumption was found to be the lowest (Figure 4.15). The lowest operational cost was also found at $Th, W_{SoC,m} = 1.5$. Figure 4.16 shows that the total operational cost was lower than Case II (a) for all the values of $Th, W_{SoC,m}$.

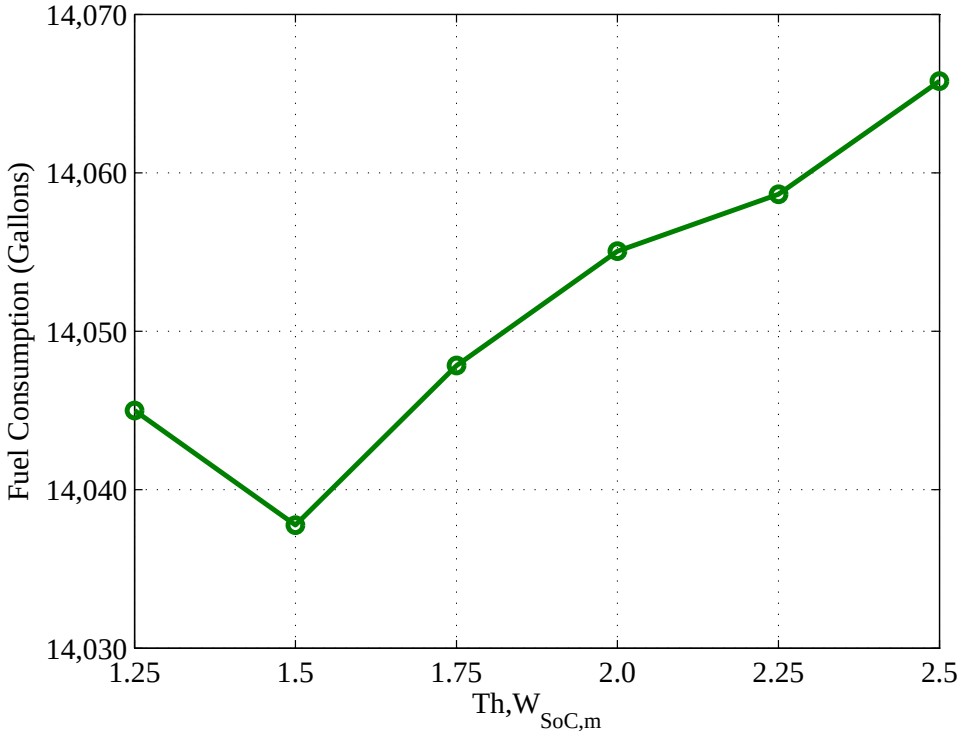

Figure 4.15. Yearly generators fuel consumption in Case II (e)

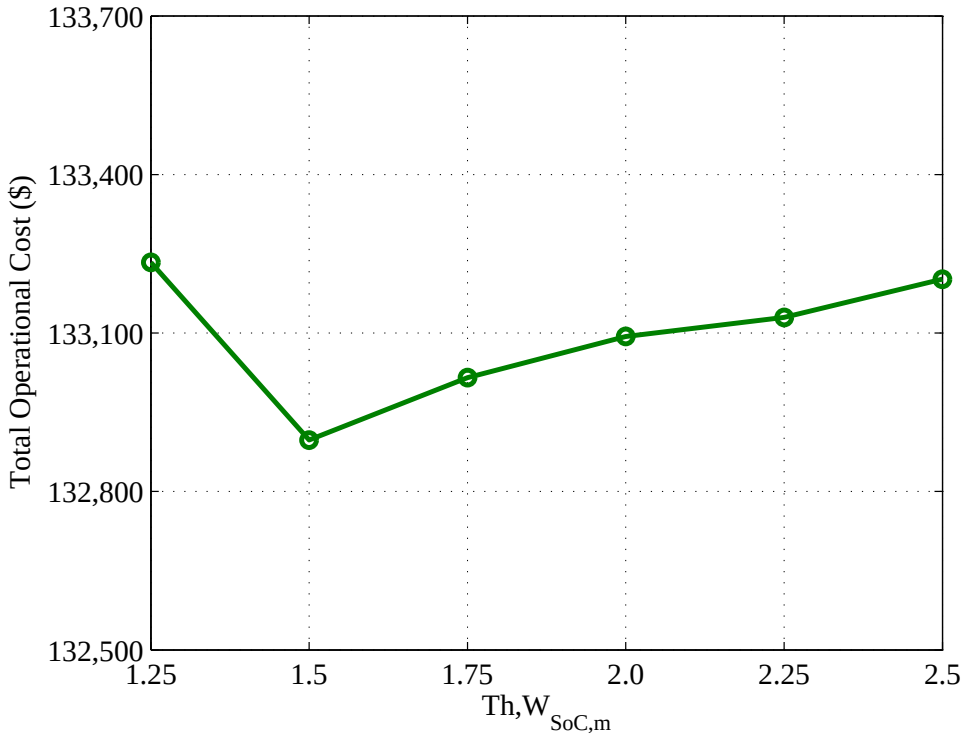

Figure 4.16. Yearly total operational cost in Case II (e)

4.3.3 Summary

According to the results, the threshold crossing charging strategy was the most cost effective over periodically charging strategy considering the operational cost and generator fuel consumption. While comparing the similar sub cases of Case I and II, results also shows that the operational cost and fuel consumption was low when $W_{SoC,m}$ was considered in the objective function. Compared to the subcases, less fuel was consumed (reduced by 82 gallons) in the Case II (e) and consequently, saved the yearly operational cost by $826 (0.62%) (Figure 4.17 and 4.18). In this part, results were compared with the Case I (a).

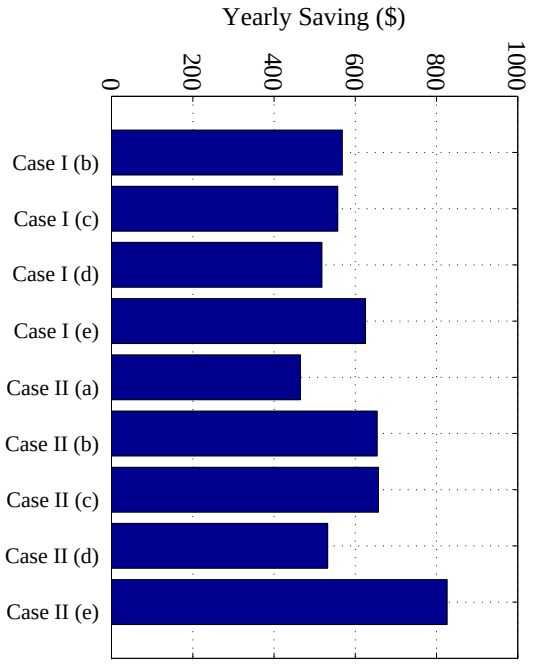

Figure 4.17. Yearly saving in different case studies

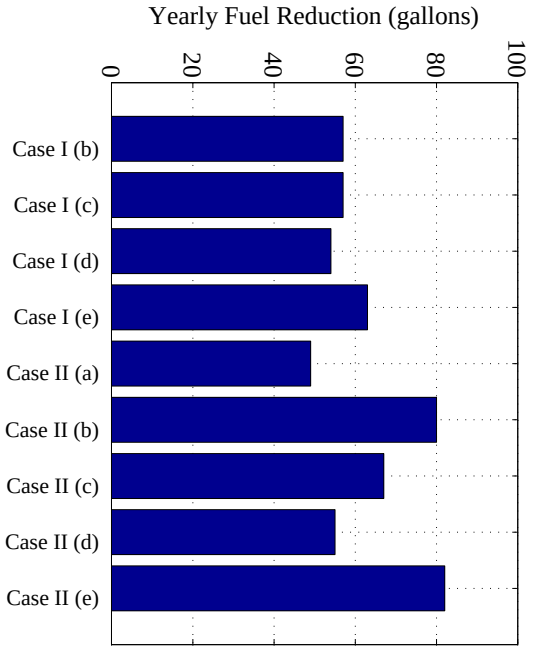

Figure 4.18. Yearly fuel reduction in different case studies

CHAPTER 5 CONCLUSIONS

Energy storage system (ESS) in remote microgrids improves the reliability and efficiency of the system. It also ensures cost-effective operation of the system by utilizing more renewable energy which are intermittent in nature. In addition, generator fuel efficiency is increased by using ESS in remote microgrids.

Lead acid (PbA) batteries are the most common energy storage system in remote microgrids due to low installation cost ($/kWh) and maintenance. But the lower life cycle and allowable depth of discharge are its main drawbacks. In recent years, lithium ion (Li-ion) and hybrid ion batteries are the immersing technologies that provide better storage solution in a sense of higher life cycle, rated DoD, operational cost, and lifetime. But the initial cost of the Li-ion battery is comparatively higher than the PbA batteries. However, ultracapacitor (UC) has 1 million life cycles, high discharging efficiency, and higher depth of discharge, although the initial cost is too high. In this thesis, the feasibility of different energy storage technologies was studied to use them in the remote microgrids energy management system (EMS). The results demonstrated that the battery wear cost is an important factor to consider while designing an EMS. It was also found that the Li-ion and hybrid ion batteries have great potentiality for remote microgrids EMS, although Li-ion battery was found to be 2.55% more cost-effective and can reduce fuel consumption by 1.5% in the system.

The operating conditions of a battery are characterized by different weight factors. Besides degrading the battery, those factors increase the system operational cost and fuel consumption in remote microgrids. To analyze the impact of those factors in the EMS, the

Schiffer Ah model was adopted in this thesis but for the sake simplicity, only SoC weighting factor was considered in the EMS. However, this model is only applicable for PbA battery. The SoC weight factor impacts the operation of remote microgrids EMS and reduces the battery life time considerably. To reduce the value of SoC weight factor, different battery charging approaches were analyzed that prevent degradation and minimize the system operational cost. Threshold crossing battery cycling strategy was found the most cost effective approach.

5.1 Conclusions

Firstly, a cost analysis of different energy storage technologies were presented for remote microgrids EMS. Result showed that the high initial cost and low energy density of UC leads towards the high operational cost. Batteries with high wear cost (PbA and $LiFePO_4$), the EMS should consider the impact on the lifetime when scheduling the batteries. The hybrid ion and Li-ion battery showed great potential for remote microgrids EMS that can lead to substantial reductions in fuel consumption.

Secondly, the impact of SoC weight factor, W_{SoC} was analyzed while PbA battery was considered as the ESS in the remote microgrid EMS. Results showed that frequent full charging of battery reduces W_{SoC}. Moreover, operation of battery at high SoC value may minimize the impact of W_{SoC}.

5.2 Future Work

The weighted Ah model is only applicable for PbA battery. Moreover, only the SoC weight factor was considered in the EMS to estimate the battery throughput and life time besides total operational cost and generators fuel consumption. Therefore, the future

works of this thesis can be to

(a) incorporate acid weight factor in the remote microgrid EMS for PbA battery.

(b) develop a general weighted Ah model for all the ESS rather than PbA battery only and implement in the remote microgrid EMS.

APPENDIX

This section presents the figures of battery weighted throughput and life time in different cases of objective 2.

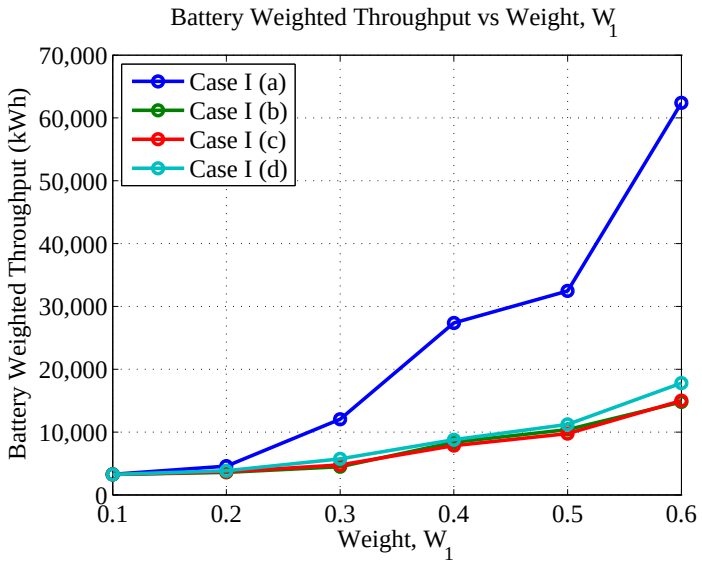

Figure .1. Yearly battery weighted throughput in Case I (a)-(d)

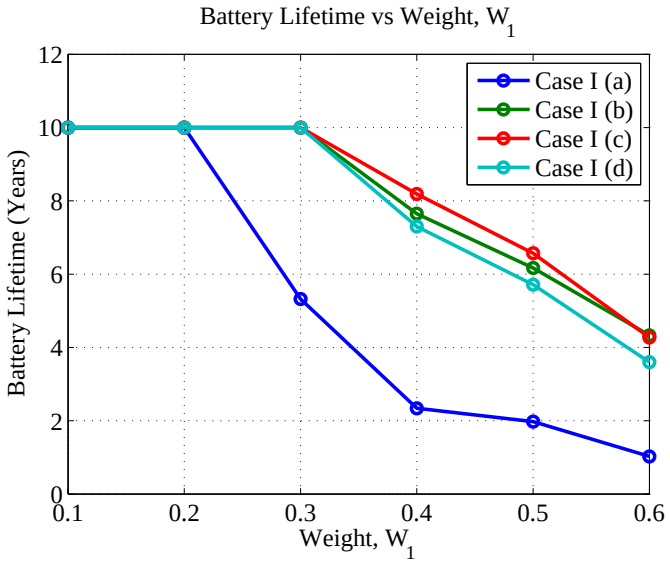

Figure .2. Battery lifetime in Case I (a)-(d)

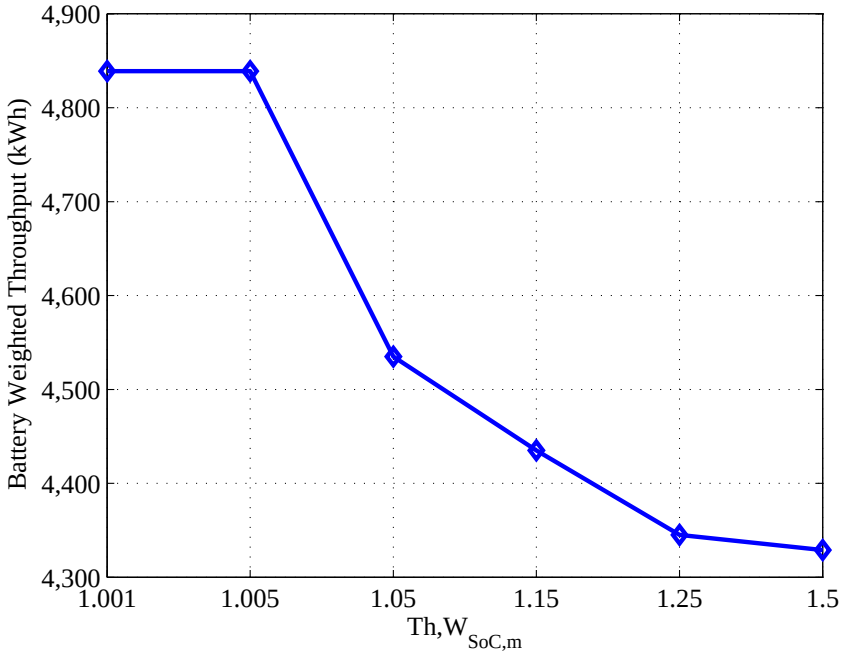

Figure .3. Yearly battery weighted throughput in Case I (e)

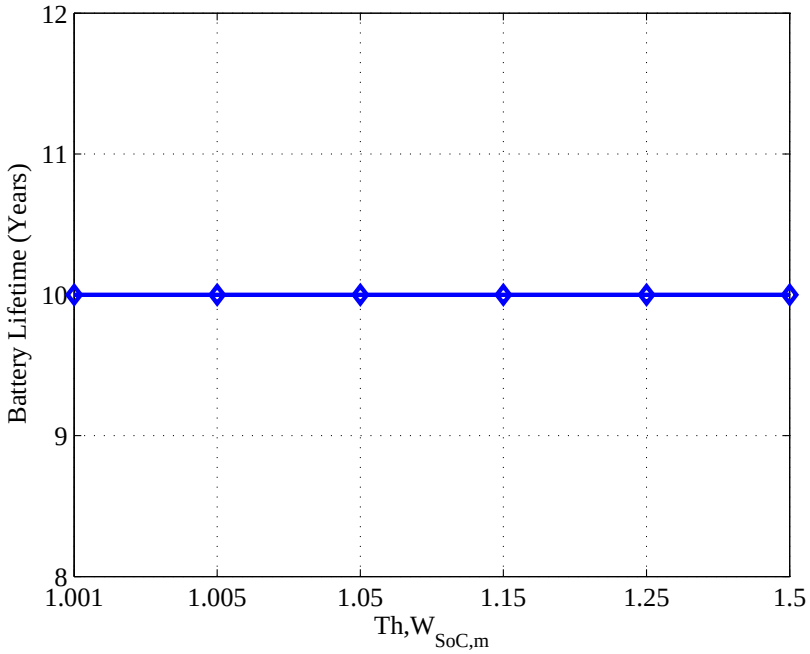

Figure .4. Battery lifetime in Case I (e)

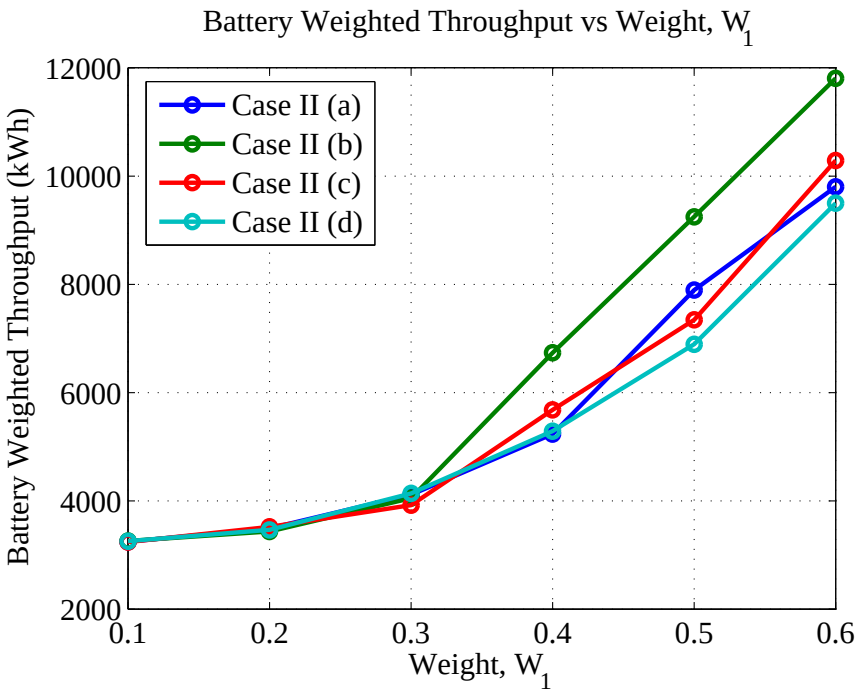

Figure .5. Yearly battery weighted throughput in Case II (a)-(d)

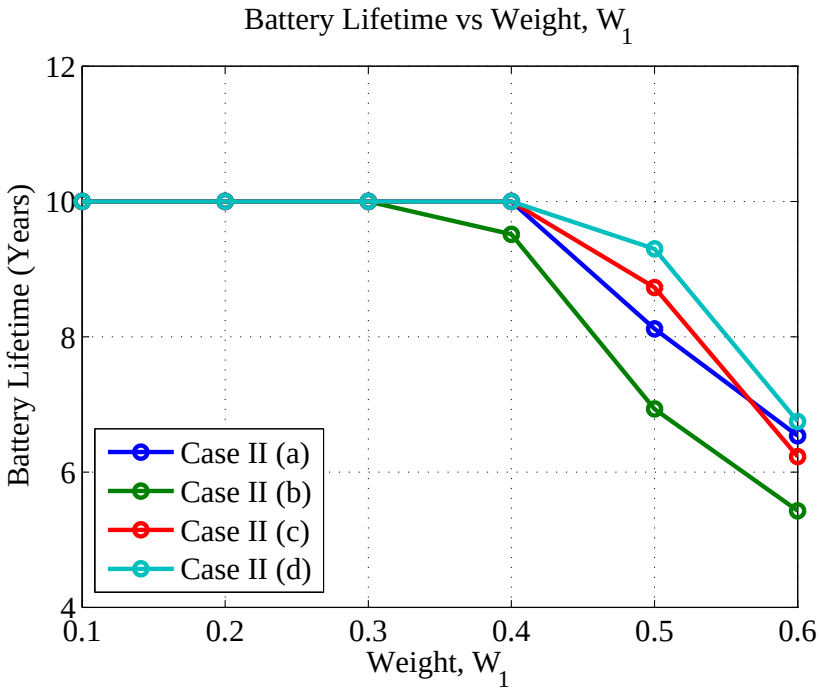

Figure .6. Battery lifetime in Case II (a)-(d)

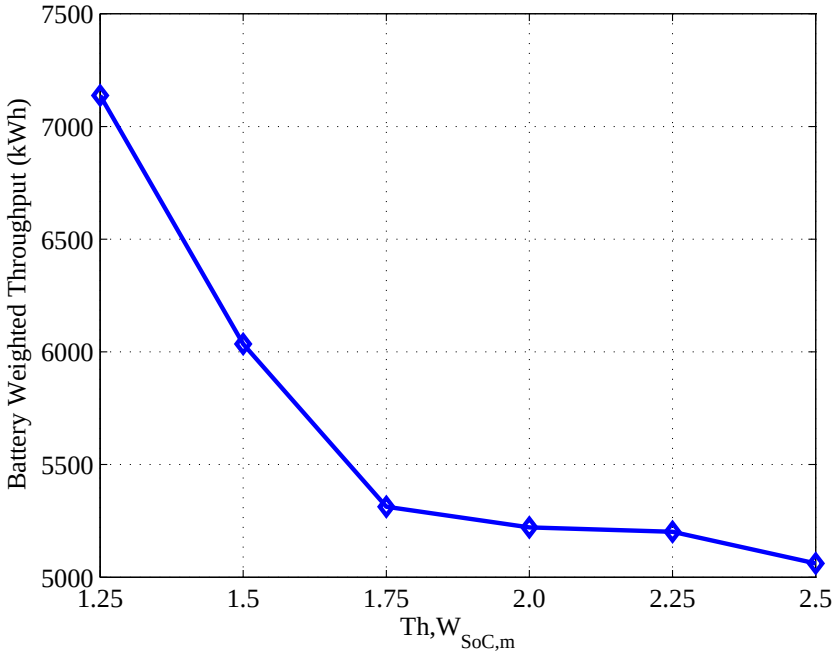

Figure .7. Yearly battery weighted throughput in Case II (e)

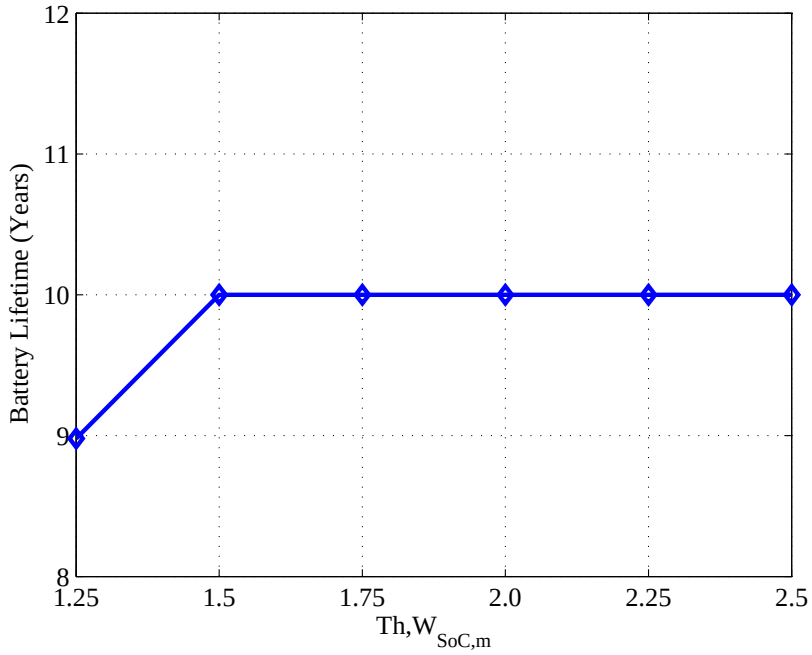

Figure .8. Battery lifetime in Case II (e)

REFERENCES

[1] B. Walsh, *Building a country by switching on the lights*, http://content.time.com/time/health/article/0,8599,2045426,00.html, [Online; Last accessed: 10 April 2016].

[2] I. E. Agency, *About energy access*, http://www.iea.org/topics/energypoverty/, [Online; Last accessed: 10 April 2016].

[3] T. Simpkins, D. Cutler, B. Hirsch, D. Olis, and K. Anderson, "Cost-optimal pathways to 75% fuel reduction in remote alaskan villages," in *Technologies for Sustainability (SusTech)*, IEEE, 2015, pp. 125–130.

[4] R. Tonkoski, "Impact of high penetration of photovoltaics on low voltage systems and remedial actions," PhD thesis, Citeseer, 2011.

[5] E. D. Tufte, "Impacts of low load operation of modern four-stroke diesel engines in generator configuration," 2014.

[6] S. Chalise and R. Tonkoski, "Day ahead schedule of remote microgrids with renewable energy sources considering battery lifetime," in *Industry Applications (INDUSCON)*, IEEE, 2014, pp. 1–5.

[7] G. Huff, *The role of storage in energy system flexibility*, https://www.iea.org/media/workshops/2014/egrdenergystorage/huff.pdf, [Online; Last accessed: 10 April 2016].

[8] U. D. of Energy, *Energy storage safety strategic plan*, http://energy.gov/oe/downloads/energy-storage-safety-strategic-plan-december-2014, [Online; Last accessed: 10 April 2016].

[9] V. Esfahanian, F. Torabi, and A. Mosahebi, "An innovative computational algorithm for simulation of lead-acid batteries," *Journal of Power Sources*, vol. 176, no. 1, pp. 373–380, 2008.

[10] M. T. Inc., *Data sheet: 48 v modules ultracapacitor*, http://www.maxwell.com/images/documents/hq_48v_ds10162013.pdf, [Online; Last accessed: 30 March 2016].

[11] K.-H. Kim, S.-B. Rhee, K.-B. Song, and K. Y. Lee, "An efficient operation of a micro grid using heuristic optimization techniques: Harmony search algorithm, pso, and ga," in *Power and Energy Society General Meeting*, IEEE, 2012, pp. 1–6.

[12] Z. Shi, Y. Peng, and W. Wei, "Optimal sizing of dgs and storage for microgrid with interruptible load using improved nsga-ii," in *Evolutionary Computation (CEC)*, IEEE, 2014, pp. 2108–2115.

[13] B. Zhao, X. Zhang, J. Chen, C. Wang, and L. Guo, "Operation optimization of standalone microgrids considering lifetime characteristics of battery energy storage system," *Sustainable Energy*, vol. 4, no. 4, pp. 934–943, 2013.

[14] P. Li, D. Xu, Z. Zhou, W.-J. Lee, and B. Zhao, "Stochastic optimal operation of microgrid based on chaotic binary particle swarm optimization," *Smart Grid*, vol. 7, no. 1, pp. 66–73, 2016.

[15] E. Hittinger, T. Wiley, J. Kluza, and J. Whitacre, "Evaluating the value of batteries in microgrid electricity systems using an improved energy systems model," *Energy Conversion and Management*, vol. 89, pp. 458–472, 2015.

[16] T. Ma, H. Yang, and L. Lu, "Feasibility study and economic analysis of pumped hydro storage and battery storage for a renewable energy powered island," *Energy Conversion and Management*, vol. 79, pp. 387–397, 2014.

[17] R. E. Ciez and J. Whitacre, "Comparative techno-economic analysis of hybrid micro-grid systems utilizing different battery types," *Energy Conversion and Management*, vol. 112, pp. 435–444, 2016.

[18] J. Schiffer, D. U. Sauer, H. Bindner, T. Cronin, P. Lundsager, and R. Kaiser, "Model prediction for ranking lead-acid batteries according to expected lifetime in renewable energy systems and autonomous power-supply systems," *Journal of Power Sources*, vol. 168, no. 1, pp. 66–78, 2007.

[19] R. Dufo-López, J. M. Lujano-Rojas, and J. L. Bernal-Agustín, "Comparison of different lead–acid battery lifetime prediction models for use in simulation of stand-alone photovoltaic systems," *Applied Energy*, vol. 115, pp. 242–253, 2014.

[20] H. Borhan, M. A. Rotea, and D. Viassolo, "Control of battery storage for wind energy systems," in *American Control Conference (ACC)*, IEEE, 2012, pp. 1342–1349.

[21] M. Y. Nguyen, D. H. Nguyen, and Y. T. Yoon, "A new battery energy storage charging/discharging scheme for wind power producers in real-time markets," *Energies*, vol. 5, no. 12, pp. 5439–5452, 2012.

[22] S. Chalise, J. Sternhagen, T. Hansen, and R. Tonkoski, "Energy management of remote microgrids considering battery lifetime," *The Electricity Journal*, 2016.

[23] I. Sanchez, *Microgrid technology: Enabling energy reliability and security – opportunities in campus, commercial and industrial communities*, http://www.districtenergy.org/assets/pdfs/03AnnualConference/Monday-A/A5.2SANCHEZIvette-Sanchez-IDEA.pdf, [Online; Last accessed: 19 April 2016].

[24] Siemens, *Microgrids*, www.siemens.com/download?DLA17_8, [Online; Last accessed: 19 April 2016], 2011.

[25] F. A. Mohamed and H. N. Koivo, "Multiobjective optimization using mesh adaptive direct search for power dispatch problem of microgrid," *International Journal of Electrical Power & Energy Systems*, vol. 42, no. 1, pp. 728–735, 2012.

[26] R. Palma-Behnke, C. Benavides, F. Lanas, B. Severino, L. Reyes, J. Llanos, and D. Sá ez, "A microgrid energy management system based on the rolling horizon strategy," *Smart Grid*, vol. 4, no. 2, pp. 996–1006, 2013.

[27] B Sedaghat, A Jalilvand, and R Noroozian, "Design of a multilevel control strategy for integration of stand-alone wind/diesel system," *International Journal of Electrical Power & Energy Systems*, vol. 35, no. 1, pp. 123–137, 2012.

[28] K. I. Elamari, "Using electric water heaters (ewhs) for power balancing and frequency control in pv-diesel hybrid mini-grids," PhD thesis, Citeseer, 2011.

[29] M. Azab, "A new maximum power point tracking for photovoltaic systems," *WASET. ORG*, vol. 34, pp. 571–574, 2008.

[30] *Power generation by renewable energy sources*, http://www.engineering.leeds.ac.uk/electronic/postgraduate/reading-list/documents/PVgenerator-1-11-12.doc, [Online; Last accessed: 19 April 2016].

[31] V. A. Chaudhari, "Automatic peak power tracker for solar pv modules using dspace r software.," PhD thesis, MAULANA AZAD NATIONAL INSTITUTE OF TECHNOLOGY, 2005.

[32] H. Energy, http://www.homerenergy.com/, [Online; Last accessed: 10 April 2015].

[33] H. Chen, T. N. Cong, W. Yang, C. Tan, Y. Li, and Y. Ding, "Progress in electrical energy storage system: A critical review," *Progress in Natural Science*, vol. 19, no. 3, pp. 291–312, 2009.

[34] R. Messenger and A. Abtahi, *Photovoltaic systems engineering*. CRC press, 2010.

[35] B. Espinar and D. Mayer, "The role of energy storage for mini-grid stabilization," 2011.

[36] K. Bradbury, "Energy storage technology review," *Duke University*, pp. 1–34, 2010.

[37] T. U. Daim, X. Li, J. Kim, and S. Simms, "Evaluation of energy storage technologies for integration with renewable electricity: Quantifying expert opinions," *Environmental Innovation and Societal Transitions*, vol. 3, pp. 29–49, 2012.

[38] J Boyes and D Menicucci, "Energy storage: The emerging nucleus," *Distributed Energy*, vol. 5, 2007.

[39] S. Suzuki, Y. Ueda, and I TAKAMITSU, "Grid stabilization for large-scale pv generation plant," in *23rd European Photovoltaic Solar Energy Conference (Valencia, Spain)*, 2008, pp. 3276–3280.

[40] R. Langella, A. Testa, and C. Ventre, "A new model of lead-acid batteries lifetime in smart grid scenario," in *Energy Conference (ENERGYCON)*, IEEE, 2014, pp. 1343–1348.

[41] V. Svoboda, H. Wenzl, R. Kaiser, A. Jossen, I. Baring-Gould, J. Manwell, P. Lundsager, H. Bindner, T. Cronin, P. Nørgård, *et al.*, "Operating conditions of batteries in off-grid renewable energy systems," *Solar Energy*, vol. 81, no. 11, pp. 1409–1425, 2007.

[42] H. Wenzl, I. Baring-Gould, R. Kaiser, B. Y. Liaw, P. Lundsager, J. Manwell, A. Ruddell, and V. Svoboda, "Life prediction of batteries for selecting the technically most suitable and cost effective battery," *Journal of power sources*, vol. 144, no. 2, pp. 373–384, 2005.

[43] D. Witmer and S. Watson, "Rural energy conference project," University of Alaska, Tech. Rep., 2008.

[44] S. Pelland, D. Turcotte, G. Colgate, and A. Swingler, "Nemiah valley photovoltaic-diesel mini-grid: System performance and fuel saving based on one year of monitored data," *Sustainable Energy*, vol. 3, no. 1, pp. 167–175, 2012.

[45] M Zivic Djurovic, A Milacic, and M Krsulja, "A simplified model of quadratic cost function for thermal generators," *Annals and Proceedings of DAAAM International*, vol. 23, no. 1, 2012.

[46] T. A. Loehlein, "Maintenance is one key to diesel generator set reliability," *Power Topic*, vol. 7004, 2007.

[47] A. Woodruff, *An economic assessment of renewable energy options for rural electrification in Pacific Island countries*. SOMAC, 2007.

[48] W. Su, J. Wang, and J. Roh, "Stochastic energy scheduling in microgrids with intermittent renewable energy resources," *Smart Grid*, vol. 5, no. 4, pp. 1876–1883, 2014.

[49] S. Drouilhet, B. L. Johnson, *et al.*, "A battery life prediction method for hybrid power applications," in *AIAA Aerospace Sciences Meeting and Exhibit*, 1997.

[50] *Technical manual for sun xtender battery*, http://www.sunxtender.com/pdfs/Sun_Xtender_Battery_Technical_Manual.pdf, [Online; Last accessed: 25 November 2015].

[51] *Sun xtender pvx-2580l agm sealed battery*, http://www.solar-electric.com/concorde-sunxtender-pvx-2580l.html, [Online; Last accessed: 25 November 2015].

[52] *Nanophosphate® lithium ion prismatic pouch cell: Amp20m1hd-a*, https://www.buya123products.com/goodsdetail.php?i=8, [Online; Last accessed: 25 November 2015].

[53] *Tesla powerwall*, http://www.teslamotors.com/powerwall, [Online; Last accessed: 25 November 2015].

[54] Z. Shahan, *38,000 tesla powerwall reservations in under a week (tesla / elon musk transcript)*, http://cleantechnica.com/2015/05/07/38000-tesla-powerwall-reservations-in-under-a-week-tesla-elon-musk-transcript/, [Online; Last accessed: 25 November 2015].

[55] *Aquion energy s20p pre-wired battery stack- 48v*, https://www.altestore.com/store/deep-cycle-batteries/batteries-saltwater-technology/aquion-energy-s30-pre-wired-26kwh-battery-stack-48v-p11941/, [Online; Last accessed: 30 March 2016].

[56] *Mouser electronics. mouser part: 723-bmod0165p048*, http://www.mouser.com/search/refine.aspx?Ntk=P_MarCom&Ntt=107638639, [Online; Last accessed: 25 November 2015].

[57] D. Jenkins, J Fletcher, and D. Kane, "Lifetime prediction and sizing of lead-acid batteries for microgeneration storage applications," *Renewable Power Generation*, vol. 2, no. 3, pp. 191–200, 2008.